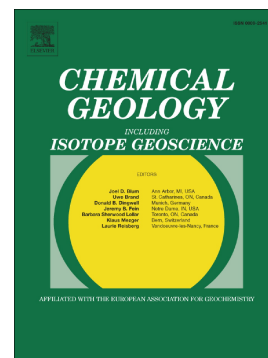


Accepted Manuscript

The noble gas isotope record of hydrocarbon field formation time scales

Igor N. Tolstikhin, Chris J. Ballentine, Boris G. Polyak, Edward M. Prasolov, Olga E. Kikvadze



PII: S0009-2541(17)30544-2
DOI: doi:[10.1016/j.chemgeo.2017.09.032](https://doi.org/10.1016/j.chemgeo.2017.09.032)
Reference: CHEMGE 18487

To appear in: *Chemical Geology*

Received date: 15 March 2017
Revised date: 16 September 2017
Accepted date: 22 September 2017

Please cite this article as: Igor N. Tolstikhin, Chris J. Ballentine, Boris G. Polyak, Edward M. Prasolov, Olga E. Kikvadze, The noble gas isotope record of hydrocarbon field formation time scales. The address for the corresponding author was captured as affiliation for all authors. Please check if appropriate. Chemge(2017), doi:[10.1016/j.chemgeo.2017.09.032](https://doi.org/10.1016/j.chemgeo.2017.09.032)

This is a PDF file of an unedited manuscript that has been accepted for publication. As a service to our customers we are providing this early version of the manuscript. The manuscript will undergo copyediting, typesetting, and review of the resulting proof before it is published in its final form. Please note that during the production process errors may be discovered which could affect the content, and all legal disclaimers that apply to the journal pertain.

The noble gas isotope record of hydrocarbon field formation time scales

Igor N. Tolstikhin

Geological Institute, Kola Scientific Center, Apatity 184209, and Space Research Institute, Moscow 117997, Russian Academy of Sciences, Russia (igor.tolstikhin@gmail.com)

Chris J. Ballentine

Department of Earth Sciences, University of Oxford, South Parks Road, Oxford, OX1 3AN, UK

Boris G. Polyak

Geological Institute, Russian Academy of Sciences, Moscow 119017, Russia

Edward M. Prasolov

St. Petersburg State University 199034 and A.P.Karpinsky Russian Geological Institute (VSEGEI) 199106, St. Petersburg, Russia

Olga E. Kikvadze

Geological Institute, Russian Academy of Sciences, Moscow 119017, Russia

Abstract

Noble gases may be considered as the most prominent tracers of natural fluids, including hydrocarbons. The atmosphere is the only source of ^{20}Ne , ^{36}Ar , ^{84}Kr , ^{130}Xe in subsurface environments, and their concentrations in pore waters after recharge are known from the solubility data. This allows modeling of noble gas partitioning between coexisting gas, oil and water phases in the course of hydrocarbon formation, migration, and storage. Radiogenic isotopes, $^4\text{He}^*$, $^{21}\text{Ne}^*$, $^{40}\text{Ar}^*$, $^{136}\text{Xe}^*$, after being released from source rocks, are mixed with air-derived noble gases already present in the pore space. Concentrations of radiogenic species in the pore space of “typical” hydrocarbon fields are generally so high, that they can hardly be accumulated *in situ* and thus indicate noble gas transfer from ground waters. The time bearing ratios $^4\text{He}^*/^{20}\text{Ne}$, $^{21}\text{Ne}^*/^{20}\text{Ne}$, $^4\text{He}^*/^{40}\text{Ar}_{\text{AIR}}$, $^{40}\text{Ar}^*/^{40}\text{Ar}_{\text{AIR}}$ in hydrocarbon fields are thus proportional to the time interval between the ground water recharge and noble gases partitioning into the hydrocarbon phase(s), the ‘recharge – partition interval’. The largest available data set allows the recharge-partition intervals to be constrained for a large number of hydrocarbon fields, situated in different tectonic settings (ancient plates, young plates, mobile belts). These intervals increase systematically with the ages of hydrocarbon source and trap lithologies and are comparable with these ages. This important feature, valid *in general* for different hydrocarbon fields, implies: (i) local sources of radiogenic noble gas isotopes in ground waters; (ii) relatively recent formation of hydrocarbon fields and (iii) their short formation time scales.

In some cases the duration of formation of a hydrocarbon field can be constrained. For example, nearly constant $^{21}\text{Ne}^*/^{20}\text{Ne}$, $^{40}\text{Ar}^*/^{40}\text{Ar}_{\text{AIR}}$ ratios, measured in samples from the Magnus oil field (North Sea), give an accumulation time scale ≈ 10 Ma. It should be emphasized that the above noble gas isotope ratios give the time estimates, which are independent of geological reconstructions.

Sometimes the noble gas inventory in a hydrocarbon field and ground waters allows characterization of the source rock volume, involved in formation of the field; generally this volume exceeds that of the hydrocarbon field rocks by orders of magnitude.

Components: 12456 words, 8 figures, 1 table.

Keywords: noble gas isotopes, hydrocarbons, ground water, partitioning, fractionation, time scales,

Index terms: 1040 Geochemistry: Isotopic composition/chemistry

Article history: Received XXX; Received in revised form XXX; Accepted XXX; Available on line XXX.

1. Introduction: Noble gas isotopes in ground waters

With our present state of knowledge, the classification of terrestrial noble gases might include many different sources and domains that host them. However, for the sake of simplicity and with a hope that this simplification will not affect substantially discussion of our major subject, time scales derived from noble gas abundances in hydrocarbon accumulations, we consider here the two dominant sources, the continental crustal rocks and the atmosphere.

Generally atmospheric noble gases are transferred into the subsurface by air saturated water (ASW), either by aquifer recharge or during burial of surface rocks bearing air saturated pore waters (e.g., Bosch and Mazor, 1988; Ballentine et al., 1991, 1996; Hiyagon and Kennedy, 1992; Aeschbach-Hertig et al., 2008; Prinzhofer, 2013; Barry et al., 2016). Even though some fractionation and degassing / ingassing processes take place at recharge, the “initial” concentrations of air saturated noble gases (^{20}Ne , ^{36}Ar , ^{84}Kr , ^{132}Xe) in ground (or pore) waters can be reasonably well constrained from the solubility data and some (generally not large) contribution from air in excess of the solubility limits. This contribution can be estimated by using concentrations of all air-derived noble gases in ground water samples (e.g. Ballentine and Hall, 1999; Peeters et al., 2002; Aeschbach-Hertig et al., 2008).

After being produced in a mineral, radiogenic noble gas isotopes (we include in this term nucleogenic and fission isotopes, e.g., $^{21}\text{Ne}^*$, $^{136}\text{Xe}^*$) are partially retained within the mineral and partially released into a pore water. Comparison of apparent whole-rock $^{238}\text{U} - ^{235}\text{U} - ^{232}\text{Th} - ^4\text{He}^*$ and $^{40}\text{K} - ^{40}\text{Ar}^*$ ages with those known from e.g. $^{87}\text{Rb} - ^{87}\text{Sr}$ or U-Th-Pb isochron dating (for about 60 samples, Tolstikhin, 1985) allows the loss parameter L (L = fraction of radiogenic atoms released from a host rock into pore space divided by the total amount produced) to be constrained. For $^4\text{He}^*$ the loss parameter, L_4 , is generally quite high, > 0.9 , whereas for $^{40}\text{Ar}^*$ L_{40} was found to be ≈ 0.4 (see Footnotes to Table 1). These values are likely to vary depending on the dominant mineral type and thermal history of the system investigated (Ballentine and O’Nions, 1994; Baxter, 2003).

Measurable concentrations of U and Th in a rock along with He concentrations in the rock – pore-water (gas, oil) system in principle allow the He residence time in this system to be quantified. To apply such simplest modelling, expressed by Eqns (1-4) below, the following assumption should be taken into account: i) there has been no gain / loss of radioactive parent isotopes into or from the rock, and ii) the radiogenic species generated in the water-bearing rocks is the only source of radiogenic noble gas species present in the rock-water system.

These assumptions are in many cases valid for the U-Th- $^4\text{He}^*$ system, especially if a helium flux from external sources can be ruled out (e.g., Lehmann et al., 2003; Tolstikhin et al., 2011; Holland et al., 2013) or constrained (e.g., Solomon, 1996). However $^{40}\text{Ar}^*$ is retained by the source minerals substantially better than $^4\text{He}^*$ and an essential $^{40}\text{Ar}^*$ fraction may have survived the weathering / sedimentation processes; therefore only partial loss of $^{40}\text{Ar}^*$ atoms generates the time-bearing signal in the pore space. These complications make the respective time scales less certain; however, consideration of predicted $^4\text{He}^*/^{21}\text{Ne}^*/^{136}\text{Xe}^*$ production (e.g. Holland et al., 2013) or the combined study of the host rocks (minerals) and related ground (pore) waters (e.g., Tolstikhin et al., 2011) allows

the noble gas mobility and losses to be constrained and thus obtain a more reliable time estimates. Such studies should be considered as an important direction of our future efforts in understanding time scales related to ground water flow, hydrocarbon production rates and hydrocarbon accumulation and evolution.

1.1. Relating in-situ noble gas production rates to ASW noble gases

For relatively young (< 300 Ma old) rocks the radiogenic $^4\text{He}^*$ produced and released into the pore water, $^4\text{He}^*_{\text{PS}}$ [mol cm⁻³] and the residence time T [years], during which He has accumulated in the pore water [ϕ is the porosity] via the decay of U and Th [$\mu\text{g g}^{-1}$] in a host rock [with the rock density ρ , g cm⁻³] are related as (e.g., Zartman et al., 1961)

$$^4\text{He}^*_{\text{PW}} \approx (5.40 \times 10^{-18} \text{ U} + 1.28 \times 10^{-18} \text{ Th}) \times T \times L \times \rho \times (1 - \phi) / \phi \quad (1a)$$

Values of the “Loss” coefficient L (defined above) are presented in the Footnotes to Table 1. For ancient samples with an age exceeding ≈ 300 Ma, the exponential decay of the parent isotopes should be taken into account. For U-Th- ^4He systematic Eqn 1a is translated into

$$^4\text{He}^*_{\text{PW}} = [8 \times ^{238}\text{U} (\text{Exp}(\lambda_{238} T) - 1) + 7 \times ^{235}\text{U} (\text{Exp}(\lambda_{235} T) - 1) + 6 \times ^{232}\text{Th} (\text{Exp}(\lambda_{232} T) - 1)] \times L \times \rho \times (1 - \phi) / \phi \quad (1b)$$

In Eqn (1b) the U, Th concentrations are mol cm⁻³ of rock and $^4\text{He}^*_{\text{PS}}$ is in units of mol cm⁻³ of pore space. The exponential term should also be included in Eqn (2) and Eqns (3, 4) for K-Ar and other systematics in case of the ancient rock-water system.

Ground water flow and noble gas diffusion in a rock-water system cause mixing of the radiogenic and atmospheric noble gases (e.g., Ballentine et al., 1996; Ballentine and Sherwood Lollar, 2002), therefore concentrations of radiogenic species in ground water can be restored from the radiogenic / air-derived isotope ratios and the ASW concentrations (hereafter subscript ASW defines concentrations of air-derived noble gases in air-saturated waters). Because of the similar solubility of He and Ne, especially in the case of saline waters (Smith and Kennedy, 1983), air-derived ^{20}Ne is the best proxy for $^4\text{He}^*$. Therefore it is possible to modify Eqn (1) by dividing its left and right sides by $^{20}\text{Ne}_{\text{ASW}} = 8.5 \times 10^{-12}$ mol ml⁻¹ (solubility for 10 °C, fresh water):

$$(^4\text{He}^* / ^{20}\text{Ne}_{\text{ASW}})_{\text{PW}} = (6.35 \times 10^{-7} \text{ U} + 1.51 \times 10^{-7} \text{ Th}) \times T \times L \times \rho \times (1 - \phi) / \phi \quad (2)$$

The solubility of He and Ne vary within $\pm 10\%$ and $\pm 20\%$, respectively, depending on temperature (from 10 to 40 °C) and salinity (from fresh to sea water). As discussed below, other factors, which affect the $^4\text{He}^*$ time scales, are more significant. Therefore for the estimates presented below we neglect: (i) variations of He and Ne solubility and treat them as constants and (ii) fractionation related to noble gas partitioning between gas (oil) and water phases, i.e., $(^4\text{He}^* / ^{20}\text{Ne}_{\text{ASW}})_{\text{GAS}} \equiv (^4\text{He}^* / ^{20}\text{Ne}_{\text{ASW}})_{\text{PW}}$. A similar equation is available for $^{21}\text{Ne}^*/^{21}\text{Ne}_{\text{ASW}}$ and $^4\text{He}^*/^{40}\text{Ar}_{\text{ASW}}$ ratios, in which case the two coefficients in Eqn (2) should be replaced by 9.78×10^{-12} and 2.32×10^{-12} (for $^{21}\text{Ne}^*/^{21}\text{Ne}_{\text{ASW}}$) and 3.15×10^{-10} and 7.45×10^{-11} (for $^4\text{He}^*/^{40}\text{Ar}_{\text{ASW}}$) respectively, providing fresh 10 °C water at recharge. It should be noted that Ar solubility could vary by a factor of ≈ 2 ; this should be taken into account when $^4\text{He}^*/^{40}\text{Ar}_{\text{AIR}}$ and / or $^{40}\text{Ar}^*/^{40}\text{Ar}_{\text{AIR}}$ ratios are used for the time scale estimates (Section 3, Fig. 3, 4).

Similar to Eqn (1), concentration of $^{40}\text{Ar}^*$ in pore water [mol ml^{-1}] can be calculated for a given K concentration [g g^{-1}] following Zartman et al. (1961):

$$^{40}\text{Ar}^*_{\text{PW}} = 1.79 \times 10^{-16} K \times T \times L \times \rho \times (1 - \phi) / \phi. \quad (3)$$

Substituting the average parent element concentrations in the upper crust, $K = 0.023 \text{ g g}^{-1}$, $U = 2.7 \mu\text{g g}^{-1}$, $\text{Th} = 10.5 \mu\text{g g}^{-1}$ (Rudnick and Gao, 2003), hereafter referred to as the average crustal concentration, in Eqns (1a, 3) gives the present-day crustal $^4\text{He}^* / ^{40}\text{Ar}^*$ production ratio of 6.7. Fig. 3 below presents a comparison of this value with those observed in hydrocarbon accumulations.

Assuming the gas phase was produced by degassing of pore water and substituting $^{40}\text{Ar}_{\text{ASW}} = 1.72 \times 10^{-8} \text{ mol ml}^{-1}$ (solubility for 10°C , fresh water) into Eqn (3) gives:

$$(^{40}\text{Ar}^* / ^{40}\text{Ar}_{\text{ASW}})_{\text{GAS}} \equiv (^{40}\text{Ar}^* / ^{40}\text{Ar}_{\text{ASW}})_{\text{PW}} = 1.04 \times 10^{-8} \times K \times T \times L \times \rho \times (1 - \phi) / \phi. \quad (4)$$

In the course of hydrocarbon formation the atmospheric and radiogenic noble gases are partitioning between the water and the hydrocarbon phase(s). To discuss this episode in noble gas evolution we consider only partitioning between water and gas: the mass balance of the two phases includes the ASW “initial” concentrations of air-derived isotopes $^i\text{C}_{\text{ASW}}$ and those after gas/water separation, $^i\text{C}_{\text{GAS}}$, $^i\text{C}_{\text{WAT}}$ [mol m^{-3}], as well as the volumes of the two phases, water, W , and gas, G [m^3], as discussed by Zartman et al. (1961):

$$^i\text{C}_{\text{ASW}} W = ^i\text{C}_{\text{GAS}} G + ^i\text{C}_{\text{WAT}} W \quad (5)$$

Assuming thermodynamic equilibrium between the two phases (both at recharge and in the course of gas phase formation at depths) and using the dimensionless expression of the Henry solubility constant $^iH_{\text{SOL}}$, ($\text{mol m}^{-3} \text{H}_2\text{O}$) / ($\text{mol m}^{-3} \text{gas}$) at 1 atm then $^i\text{C}_{\text{WAT}} = ^iH_{\text{SOL}} ^i\text{C}_{\text{GAS}}$. Substituting this into Eqn (5) gives the gas / water ratio under STP conditions:

$$^iG / ^iW = ^i\text{C}_{\text{ASW}} / ^i\text{C}_{\text{GAS}} - ^iH_{\text{SOL}} \quad (6)$$

$^iG / ^iW$ ratios, calculated from ^{36}Ar and ^{84}Kr concentrations, correlate within a wide range, $0.1 \leq G / W \leq 200 \text{ m}^3/\text{m}^3$ (Fig. 1). A large number of data points shifting around the equality line indicate, that the equilibrium gas / water partitioning of noble gases between ASW and hydrocarbon phases may be considered as a reasonable approximation of formation of hydrocarbon accumulations in many natural environments (Bosch and Mazor, 1988; Ballentine et al., 1991, 1996; Hiyagon and Kennedy, 1992; Prinzhofer, 2013). The deviation from the correlation can be used as a measure of degree of the equilibrium or as evidence of other scenarios (e.g. Torgersen and Kennedy, 1999; Zhou et al., 2005; Barry et al., 2016).

Fig. 1.

In some cases partitioning of He and Ar between co-existing water and hydrocarbon phases could modify the $^4\text{He}^* / ^{40}\text{Ar}_{\text{AIR}}$ ratio due to different solubility of these species: for the gas / water ratios ≈ 0.1 the $^4\text{He}^* / ^{40}\text{Ar}_{\text{AIR}}$ ratio increases by a factor of ≈ 1.5 in the gas phase compared with the initial ratio in the ground water. However, the partitioning produces negligible effect on the ratios of radiogenic to air-derived isotope of the same elements, e.g., $^{40}\text{Ar}^* / ^{40}\text{Ar}_{\text{AIR}}$, $^{21}\text{Ne}^* / ^{21}\text{Ne}_{\text{AIR}}$. With some exceptions the low solubility of noble gases in water along with the equilibrium gas / water partitioning

provide almost complete transfer of noble gases from the ground waters into the hydrocarbon accumulations.

1.2. Using ASW and radiogenic noble gases to understand hydrocarbon systems

In this paper we emphasise rather high abundances of noble gases in hydrocarbon accumulations, situated in different tectonic settings: ancient plates, young plates and mobile belts (see Table 1 and Footnotes to this Table). The contribution of *in-situ*-generated radiogenic noble gas species appears to be negligible. The “time-bearing” ratios, $^4\text{He}^*/^{20}\text{Ne}_{\text{AIR}}$, $^4\text{He}^*/^{40}\text{Ar}_{\text{AIR}}$, $^{21}\text{Ne}^*/^{21}\text{Ne}_{\text{AIR}}$, $^{40}\text{Ar}^*/^{40}\text{Ar}_{\text{AIR}}$, $^{136}\text{Xe}^*/^{136}\text{Xe}_{\text{AIR}}$, were inherited from the ground waters during hydrocarbon formation, and “frozen” in the accumulations, which may be considered as “samplers” of noble gases extracted from ground waters.

The main objective of this study is using these ratios, measured in hydrocarbons, in order to constrain the ground water recharge - partitioning intervals and thus also shed light on sources of noble gases in ancient ground waters and the time scales of formation of hydrocarbon accumulations. This approach has already been applied to several hydrocarbon fields (see for example Ballentine et al., 1991, 1996; Hiyagon and Kennedy, 1992; Pinti and Marty, 1995, 2000; Barry et al., 2016).

Here we use a large data set on He and Ar isotope abundances in hydrocarbon accumulations, compiled in Table 1, in order to show some *general* features of hydrocarbon field formation, traced by noble gas isotopes, *i.e.*, (i) to reveal the sources of noble gas species in hydrocarbon fields, situated in different tectonic settings, *i.e.*, the ground waters, and to constrain their recharge – partition intervals; (ii) to compare durations of these intervals with the stratigraphic ages of respective source and trap rocks and constrain hydrocarbon field formation time scales; it is important to note, that these time constraints are independent on petrochemical modelling of hydrocarbon systems; (iii) to estimate volumes of ground waters, required to fill the hydrocarbon fields, and the rates of hydrocarbon formation.

2. Abundances of radiogenic noble gas isotopes in hydrocarbon accumulations

It should be emphasized that high abundances of radiogenic $^4\text{He}^*$, $^{21}\text{Ne}^*$ and $^{40}\text{Ar}^*$ in the pore space of rocks hosting “typical” hydrocarbon fields can hardly be accumulated *in situ* from the average concentrations of the parent radioactive elements, even assuming that the rock – hydrocarbon-fluid system has been “closed”: *i.e.* no loss or gain of the species of interest since the formation of trap rocks.

In order to confirm this important issue, we assume the depth of an average hydrocarbon accumulation, 1500 m, the temperature, 45 °C, the trap rock density 2.7 g cm⁻³ and the porosity, 0.2. Then the average concentration of $^4\text{He}^* = 1.250 \times 10^{-3}$ in accumulations, situated in the ancient plates, corresponds to $^4\text{He}^*$ amount in the host rocks, 1.43×10^{-6} mol cm⁻³ (Table 1). Providing the average crustal concentrations U and Th in these rocks (Footnotes to Table 1), then the age, required to generate such $^4\text{He}^*$ amount, 6300 Ma, would be well above the Earth’s age and by a factor of ≈ 20 exceeds the average stratigraphic ages of the hydrocarbon source and trap rocks (line 1 in Table 1). This is also valid for hydrocarbon accumulations situated in other tectonic settings (lines 2 and 3 in Table 1). $^4\text{He}^*$ amounts in the trap rocks can also be derived from relatively constant partial pressure of $^{40}\text{Ar}_{\text{AIR}}$ and the ratios of $^4\text{He}^*/^{40}\text{Ar}_{\text{AIR}}$, available for different tectonic settings (Table 1). This approach also gives the meaningless long accumulation ages: 4000, 2000 and 380 Ma for the ancient plates, young plates and mobile belts, respectively.

Data available in Table 1 allow independent estimate of the “accumulation ages” via the “field” concentrations of $^4\text{He}^*$ (col. 15), the $^4\text{He}^*/^{40}\text{Ar}^*$ ratio (col. 11), and the average crustal concentration

of potassium (Footnote ‘c’ to Table 1): the apparent K-Ar ages, required to produce the $^{40}\text{Ar}^*$ in the pore space of the trap rocks, approach [Ma] 6700, 2000 and 490 for the ancient plates, young plates and mobile belts, respectively, also greatly exceeding the ages of the trapping lithologies.

According to these estimates, noble gases in the pore space of hydrocarbon bearing rocks could only be sourced from a large volume of pore water (Fig. 2). These general relationships are in accord with results discussed in the literature for several hydrocarbon accumulations even though in some cases fluxes of species from external sources are also observed; examples are presented in Section 5.2.

Summarizing, hydrocarbon accumulations generally shows high concentrations of ground water derived ASW and radiogenic noble gases. The accumulations work as giant natural “samplers”, preserving the noble gases as well as their time-bearing isotopic ratios of $^4\text{He}^*/^{20}\text{Ne}_{\text{AIR}}$, $^4\text{He}^*/^{40}\text{Ar}_{\text{AIR}}$, $^{21}\text{Ne}^*/^{21}\text{Ne}_{\text{AIR}}$, $^{40}\text{Ar}^*/^{40}\text{Ar}_{\text{AIR}}$, which can be translated into the recharge – partitioning time intervals, important parameters highlighting sources of noble gases in ancient waters and hydrocarbon formation time scales, as discussed in Section 3. Moreover, not only hydrocarbon fields but most terrestrial gases are characterised by rather high noble gas concentrations (for example He) well above those observed in ground waters (Fig. 2).

Table 1 .

Fig. 2.

3. Recharge – partition intervals and hydrocarbon field formation time scales

3.1. The recharged partition intervals derived from $^4\text{He}^/^{40}\text{Ar}_{\text{ASW}}$ and $^{40}\text{Ar}^*/^{40}\text{Ar}_{\text{ASW}}$ ratios in hydrocarbon accumulations.*

Several processes are not taken into account by Eqns (2, 4).

- (1) Mixing of ground waters with different ratios of radiogenic / stable isotopes or an external flux of radiogenic isotopes, so that the radiogenic / stable isotope ratios do not indicate “aging” of the rock / water system as envisaged by Eqns (2, 4), but instead then represent a mixing process (e.g., Marine, 1979; Hiyagon and Kennedy, 1992; Ballentine and Sherwood-Lollar, 2002). In some cases additional data can help to resolve this dilemma for ground water dating (e.g., Tolstikhin et al., 2011).
- (2) After the hydrocarbon field has been formed, the gas phase can interact with underlying ground water (e.g., Zhou et al., 2005, 2012; Gilfillan et al., 2008, 2011). The gases partitioning into the gas field at that late stage include both air-derived and radiogenic isotopes. Depending on the composition of these “post-gas-field-formation” injections the calculated recharge-partition interval can deviate from formation values.
- (3) After an early stage of hydrocarbon formation, such as low temperature microbial methanogenesis, the lithology containing the (already degassed) ground water can be buried further during basin evolution. This ground water will contain low concentrations of air-derived and radiogenic noble gases with the fractionated abundance pattern. The deficit of air-derived ^{20}Ne relative to ASW concentrations could cause a large increase in the $^4\text{He}^*/^{20}\text{Ne}$ and $^{21}\text{Ne}^*/^{20}\text{Ne}$ ratios even in case of low contributions of radiogenic $^4\text{He}^*$ and $^{21}\text{Ne}^*$; this is also true for other radiogenic / air derived noble gas isotope ratios. If the noble gases are partitioned between this “fossil” water and hydrocarbon phases in the next hydrocarbon forming event, the ratios would indicate an excessive recharge – partition interval. Strong fractionation of noble gases is indeed rarely observed, as it follows from Fig. 1 and related Text. In a large data base available to Prinzhofer (2013) only one sample with unusually high ratios $^{84}\text{Kr}/^{20}\text{Ne} = 1.5$ and $^{36}\text{Ar}/^{20}\text{Ne} = 22$ has been identified ($^{84}\text{Kr}/^{20}\text{Ne}$ and $^{36}\text{Ar}/^{20}\text{Ne}$ in air are 0.0395 and 1.91, respectively). Also Verchovsky et al. (1988) observed the fractionation parameter $(^{130}\text{Xe}/^{40}\text{Ar}_{\text{AIR}})_{\text{SAMPLE}} / (^{130}\text{Xe}/^{40}\text{Ar})_{\text{AIR}}$ up to 14 and $(^{84}\text{Kr}/^{40}\text{Ar}_{\text{AIR}})_{\text{SAMPLE}} / (^{84}\text{Kr}/^{40}\text{Ar})_{\text{AIR}}$ up

to 4 in the deepest segments of the Urengoi field, in a qualitative agreement with the lowest abundance of $^{40}\text{Ar}_{\text{AIR}}$ in this segment. However these authors had not considered a possibility of transfer of atmospheric heavy noble gases by coal-bearing rocks (e.g., Zhou et al., 2005).

Though the above list of problems looks pessimistic, the processes which control some individual hydrocarbon systems can be recognised and their effects quantified (e.g. Pinti and Marty, 1995; Zhou et al., 2005; Barry et al., 2016; Sathaye et al., 2016). Also in spite of these complications the *general “age” effect* is directly visible as an increase in the ratio of radiogenic to air-derived noble gas isotopes with the age of the hydrocarbon trap rocks (reservoirs). Low $^4\text{He}^*/^{40}\text{Ar}_{\text{ASW}}$ and $^{40}\text{Ar}^*/^{40}\text{Ar}_{\text{ASW}}$ ratios are typical of hydrocarbon fields situated in “young” tectonically active regions (e.g., Sakhalin, Japan, see Footnotes to Table 1). Intermediate values characterize fields of the post-Hercynian plates (e.g., West-Siberian, Scythian, Turanian). Hydrocarbon fields from ancient Precambrian platforms (e.g., East-Siberian and East-European) show the highest $^4\text{He}^*/^{40}\text{Ar}_{\text{ASW}}$ and $^{40}\text{Ar}^*/^{40}\text{Ar}_{\text{ASW}}$ ratios. A reasonably good correlation between $^{40}\text{Ar}^*/^{40}\text{Ar}_{\text{ASW}}$ and $^4\text{He}^*/^{40}\text{Ar}_{\text{ASW}}$ for a number of hydrocarbon fields illustrates that both systems work self-consistently (Fig. 3). This “expected” behaviour of noble gas species stimulates an apparent qualitative interpretation: transfer of the time bearing isotope ratios into the recharge - partition time intervals and comparison of these intervals with the time scales typical for given tectonic setting.

Fig. 3.

Substituting $^4\text{He}^*/^{40}\text{Ar}_{\text{AIR}}$ ratios, shown in Table 1, into Eqn (2, 4) gives the following time intervals between (fresh, 10 °C) ground water recharge and noble gas partitioning into hydrocarbons phase(s): 400, 165 and 28 Ma for hydrocarbon fields on the ancient plates, young plates and in tectonically active regions, respectively. In case of recharge of warm (40 °C) salty (40 permil) water Ar solubility decreases by a factor of ≈ 2 (Weiss, 1970); in this case the time scales would be reduced by a factor of two, giving the average values of 300, 120 and 22 Ma; these values are presented in col. 14, Table 1.

$^{40}\text{Ar}^*/^{40}\text{Ar}_{\text{AIR}}$ ratios give the same relative time sequence, but shorter absolute time scales, for example 175 Ma for the ancient plates. The different behaviour of $^4\text{He}^*$ and $^{40}\text{Ar}^*$ in crustal rocks (Section 1) readily explains this discrepancy: $^{40}\text{Ar}^*$ is better preserved in “cold” environments (with temperature gradient $\approx 30\text{ }^\circ\text{C km}^{-1}$), therefore the loss coefficient in Eqn (4) plays an important role. Assuming the loss coefficient $L_{40} \approx 0.5$ for “cold” ancient plates, ≈ 0.7 for young plates and 1 for tectonically active regions, then the ^{40}K - $^{40}\text{Ar}^*$ - $^{40}\text{Ar}_{\text{AIR}}$ systematics gives similar recharge-partition ages for the three tectonic settings as derived above from the U-Th- $^4\text{He}^*$ - $^{40}\text{Ar}_{\text{AIR}}$ data. The above estimates of the loss parameter are in a qualitative accord with the $^4\text{He}^*/^{40}\text{Ar}^*$ ratios in the three hydrocarbon accumulation environments (Table 1): this ratio in tectonically active regions is below the production ratio (Section 1.2), thus indicating a substantial loss of radiogenic $^{40}\text{Ar}^*$, whereas three times higher ratios in ancient plates implies a better retention of this nuclide. Fig. 3 illustrates a reasonable agreement between durations of the recharge partition intervals derived from the ^{40}K - $^{40}\text{Ar}^*$ - $^{40}\text{Ar}_{\text{AIR}}$ and U-Th- $^4\text{He}^*$ - $^{40}\text{Ar}_{\text{AIR}}$ systematics.

3.2. The recharged partition intervals and ages of the source and trap rocks: a comparison.

The above time estimates seem reasonable, as they do reflect the chronology of the respective geological environments: the average ages of hydrocarbon trap rocks on the ancient plates, young plates and in mobile belts, presented in Table 1, amounts to 320 Ma 130 Ma and 35 Ma, respectively, (Fig. 4).

Fig. 4.

The noble gases are mainly partitioned between ground waters and hydrocarbon phases: (i) in the course of hydrocarbon generation within source rocks and (ii) during hydrocarbon migration from these rocks through overlaying strata into a trap structure. Therefore the recharge – partition intervals should be compared with the stratigraphic intervals containing hydrocarbon source rocks. These intervals are not available in our data set (Table 1). However, because we consider the data in Table 1 to be representative for the world hydrocarbon systems, the world wide source rock chronology, compiled from the literature, may be used for the comparison. Such detailed compilation was presented by Klemme and Ulmishek (1991) and Fig. 5 shows that relationships between the recharge – partition intervals and the source rock ages are very similar to those seen in Fig. 4 for the trap rocks. This is an expected result as the age differences between the source and trap rocks are generally small. For example, 25 % of the world hydrocarbon resources were produced in the Upper Jurassic and 14 % were preserved in trap rocks of the same age interval: difference between the sedimentation ages of the source and trap rocks is within ≈ 25 Ma and cannot be resolved (Fig. 5) by not precise noble gas chronometry. These close sedimentation ages of the source and trap rocks are typical for the whole Phanerozoic (see Fig. 16 in Klemme and Ulmishek, 1991). As discussed below the filling of structural traps generally occurred well after the sedimentation.

Fig. 5.

3.3. Relatively “young” ages of the hydrocarbon accumulations

The similarity between the duration of the recharge-partition intervals and the ages of the source and trap rocks (Fig. 4, 5) sheds light on the chronology of the hydrocarbon production / filling processes. The most straightforward and simple explanation of this similarity envisages *formation* of the (source and trap) *rocks* within a short time interval (Fig. 16 in Klemme and Ulmishek, 1991) and *simultaneous recharge* of the related ground *waters*, for example ≈ 300 Ma ago for the ancient plates (col. 13 and 14 in Table 1). Hydrocarbons were continuously generating, releasing from the source rocks and migrating to the Earth’s surface (thus producing hydrocarbon fluxes from “geological sources”), while radiogenic noble gas isotopes were accumulating in the pore waters, migrating towards the hydrocarbon generating domain. The structural traps (e.g., the anticlines, salt domes, their combination, etc.) had been formed and filled by hydrocarbon materials *relatively recently*, as recorded by partitioning of noble gases from the *ancient waters* into hydrocarbon phases. Indeed in case of very early filling of a hydrocarbon field (e.g., ≈ 300 Ma ago, assuming the trapping and seal lithologies and the trap structure were formed at that early time), the field should contain noble gases with rather low ratios of radiogenic over ASW species.

To illustrate a possibility of recent fast filling of a hydrocarbon field, we consider the present day average methane flux through the continental area. This flux took place if hydrocarbons are generated within the source rocks and expelled into overlaying strata, but the trap structure has not been formed yet; in this case hydrocarbons migrate through tectonic dislocations to the earth surface. Etiope et al. (2008) derived the average methane flux, emitted from the geologic sources into the atmosphere, between $(2 \text{ and } 4) \times 10^{-2} \text{ mol m}^{-2} \text{ a}^{-1}$.

Independent estimate of this flux follows from the $\text{CH}_4 / {}^4\text{He}^*$ ratio in hydrocarbon gases and the ${}^4\text{He}^*$ flux from “geological sources”. According to a compilation by Ma et al. (2005) the average value of the latter approaches $\approx 1 \times 10^{-6} \text{ mol m}^{-2} \text{ a}^{-1}$. The methane / helium isotope plot, proposed by Welhan and Craig (1983), was later discussed by Jenden et al. (1988, 1993) and by Pinti and Marty (2000) for selected data, illustrating mixing of mantle and crustal methane / helium duo. Fig. 6

presents a much greater data set, including almost all data available in the scientific literature (Polyak et al., 2015). Even though the spread of the data points is large, Fig. 6 in principle agrees with the previous versions as it also shows mixing of crustal and mantle gases. According to this Figure, the typical crustal $\text{CH}_4 / ^4\text{He}^*$ ratio is $\approx 2 \times 10^4$. The product of $^4\text{He}^*$ flux $\times \text{CH}_4 / ^4\text{He}^*$ ratio gives the average methane flux $\approx 2 \times 10^{-2} \text{ mol m}^{-2} \text{ a}^{-1}$, in a good agreement with the value compiled by Etiope et al. (2008).

This flux could fill the giant Urengoi gas field during $\approx 1 \text{ Ma}$. A time scale of a few million years, required for accumulation of a hydrocarbon field, is short indeed relative to the stratigraphic ages of the hydrocarbon source and trap rocks in any tectonic environment as well as to the duration of the respective recharge – partition intervals (Table 1, see Section 4).

Fig. 6.

Examples of the relatively recent filling of hydrocarbon fields have been known for a long time. Thus, Pinty and Marty (1995) highlighted the similarity between noble gas isotope signatures in the Dogger aquifer and in related oil fields (the Paris Basin, France): partitioning of noble gases between ancient ground water and oil had occurred relatively recently. Important is that detailed studies of stratigraphy and tectonics of geological provinces, enriched in gas and oil resources, resulted in a similar conclusion. For example, the source rocks in the Central Arabian Paleozoic Petroleum System and Arabian Sub-Basin Petroleum System (the Greater Ghawar Province, Arabian Peninsula) are of the Early Silurian (425 Ma) and the Middle Jurassic (175 Ma) ages, respectively. However, the major tectonic events that created the traps for hydrocarbons occurred in both sites much later, mainly during two Alpine tectonic episodes, the Late Cretaceous (70 Ma) and the Late Tertiary (20 Ma), and filling of these traps took place from $\approx 40 \text{ Ma}$ till $\approx 10 \text{ Ma}$ ago (Pollastro, 2003).

From the above discussion it becomes clear, that the relatively “young” ages of the generation / expulsion / filling process is a general feature of hydrocarbon accumulations. An early filling followed by a long preservation ($\approx 300 \text{ Ma}$) of a hydrocarbon field, presented as example by Magoon and Dow (1994, see Fig. 1.5 in their paper), should be considered as an exception.

3.4. The recharge – partition time interval and the helium fluxes through the continental crust

The similarity between the duration of the recharge-partition intervals and the ages of source and trap rocks in different tectonic environments, indicates the dominantly “local” environments and the relatively “simple” fractionation processes. Such similarity is not expected if trans-continental fluxes of noble gas species were responsible for the noble gas abundances in hydrocarbon accumulations.

Rocks of the continental crust have lost almost all radiogenic *in-situ* produced He (Mamyrin and Tolstikhin, 1984). Assuming the steady state relationships between He production and loss, and taking into account the reasonably well known abundances of the parent elements (U and Th) in the crustal rocks, the hypothetical transcontinental $^4\text{He}^*$ flux, $\approx 1.5 \times 10^{-6} \text{ mol m}^{-2} \text{ a}^{-1}$ has been derived (O’Nions and Oxburgh, 1988). This value is useful for understanding an average crustal He flux into the atmosphere, for comparing observed fluxes in different localities, and also can be used for other “average” estimates, for example the methane flux, as has been done in the above Section 3.3.

The observable manifestations of the He flux from continental crustal domains are highly dependent on the local tectonic structure and vary within a wide range from $\approx 10^{-2}$ (and less) to $\approx 10^{-5} \text{ mol m}^{-2} \text{ a}^{-1}$. Therefore the average crustal value of the continental He flux can hardly be applied to any given local environment. Moreover, before applying to an external flux the local sources should be investigated carefully enough; otherwise the interpretations may be reconsidered. Well known

examples are aquifers within the Great Artesian Basin (e.g. Torgersen and Ivey, 1985) and Molasses basin, Northern Switzerland (Pearson et al., 1991). Subsequent careful studies of the radioactive element concentrations and radiogenic noble gas content in adjacent aquifer / aquitard systems show that the local environments can adequately account for the radiogenic noble gases in the Great Artesian Basin (Love et al., 2000; Lehmann et al., 2003) and in the Permian - Carboniferous sandstone/shale interlay in the Molasses Basin (Tolstikhin et al., 1996, 2011).

Because of the anomalous mobility of He, the external He fluxes should have been revealed by rather high $^4\text{He}^*/^{40}\text{Ar}_{\text{ASW}}$ ratios and $^4\text{He}^*/^{40}\text{Ar}_{\text{RAD}}$, which is in full contrast to the general characteristics of hydrocarbon fields, presented in Table 1 (column 7) and rather large volumes of ground waters sourced the fields (Section 5). This does not mean that He fluxes from depths are absent or never observed (Section 5.2, Fig. 7): they should be considered as rare events compared with accumulations of radiogenic noble gas isotopes in local environments. It should be noted that the latter term, local environments, defined crustal domain(s) below the hydrocarbon field and above the hydrocarbon source rocks.

4. Recharge – partition and oil filling intervals: the Magnus oilfield case study

As has already been mentioned, in many cases radiogenic and air-derived noble gas species have been well mixed before hydrocarbon formation. Ballentine and Sherwood Lollar (2002) noted that the duration of the hydrocarbon formation interval, including the generation of hydrocarbon phase(s) and hydrocarbon removal from the source domain, should be short: otherwise production of radiogenic isotopes during these events would result in an increase radiogenic / air derived noble gases ratios directly in the course of accumulation of a hydrocarbon field. Also some difference of the time bearing ratios in segments of a field could result from hydrocarbon supply from different sources (see Section 5). To minimize these effects, very similar isotope ratios (e.g., $^{21}\text{Ne}^*/^{21}\text{Ne}_{\text{AIR}}$ or/and $^{40}\text{Ar}^*/^{40}\text{Ar}_{\text{AIR}}$), measured in different sections of a hydrocarbon field, are required to estimate the duration of the hydrocarbon formation interval along with evidence for limited mixing after the field has been formed; the estimate would be efficient if the radiogenic to air isotope ratios ($^{21}\text{Ne}^*/^{21}\text{Ne}_{\text{AIR}}$, $^{40}\text{Ar}^*/^{40}\text{Ar}_{\text{AIR}}$) were near constant while the concentrations of the elements used (e.g., Ne or Ar) were variable.

Ballentine et al. (1996) presented such a case study: perfect mixing of radiogenic and air-derived Ar and Ne isotopes for 9 samples collected from different boreholes producing from the Magnus oilfield, North Sea (the maximum distance between the boreholes being ≈ 6 km, the depth difference ≈ 300 m). These samples present an almost constant $^{40}\text{Ar}^*/^{40}\text{Ar}_{\text{ASW}} = 0.48 \pm 0.01$ and $^{21}\text{Ne}^*/^{21}\text{Ne}_{\text{ASW}} = 0.132 \pm 0.0053$ (the average value $\pm 1 \sigma$) along with slightly variable $^4\text{He}^*/^{20}\text{Ne}_{\text{ASW}} \approx 7700$, whereas $^4\text{He}^*$, $^{40}\text{Ar}^*$ and $^{21}\text{Ne}^*$ concentrations vary within a factor of ≈ 2 , eliminating the possibility of post-field-formation mixing.

The above ratios give ≈ 100 Ma long recharge – partition interval (Fig. 4). This is in a reasonable agreement with the interval, that passed by between the age of formation of trap lithology, 150 Ma ago, and time when the trap had been filled by oil, 65 Ma ago, and the noble gas ratios were “frozen in oil”. It should be noted that this noble gas chronology is in accord with the estimates derived from geological considerations (see Ballentine et al., 1996, and references therein).

The deviation from the average values, presented above, allows the filling time interval to be constrained. Thus, the average $+ 3 \times 1 \sigma$ values are substantially outside all measured $^{40}\text{Ar}^*/^{40}\text{Ar}_{\text{ASW}}$ and $^{21}\text{Ne}^*/^{21}\text{Ne}_{\text{ASW}}$ ratios [Table 2 in Ballentine et al., 1996]. Therefore $\Delta ^{40}\text{Ar}^*/^{40}\text{Ar}_{\text{ASW}} = 3 \times 1 \sigma = 0.03$ may be considered as an “observable” effect of “aging in the course of filling”. Substituting the

latter value, K content from Ballentine et al. (1996) and other parameters from Footnote to Table 1 in Eqn (4) gives the Magnus oilfield formation interval ≈ 5 Ma.

Applying the same approach to the results of Ne isotope measurements and thus considering the observable effect as $\Delta^{21}\text{Ne}^*/^{21}\text{Ne}_{\text{ASW}} = 0.016$, then Eqn 2 (re-arranged for the above ratio with U and Th contents from Ballentine et al. 1996) gives a somewhat longer time interval, ≈ 14 Ma. Both estimates (the average value being 10 ± 5 Ma) indicate a short duration of the oil filling interval. This result is in contrast with the extended burial history of the regional hydrocarbon producing system (Johnson et al., 2005), but likely shows the rate and impact of quartz cementation formation at the base of this hydrocarbon reservoir; this formed concurrently with hydrocarbon filling, sealed the reservoir and stimulated the original noble gas investigation.

5. Noble gas isotope abundances in selected hydrocarbon accumulations and related ground waters

5.1. The bulk gas / water ratios as recorded by noble gas inventory

In Section 2 we highlighted that rather high abundances of noble gases in hydrocarbon fields is a general feature of hydrocarbon systems and ground waters are the only source of these gases; here several selected individual examples are presented. At the beginning we consider the $^{40}\text{Ar}_{\text{AIR}}$ balance in the largest Cenomanian field of the giant Urengoi gas deposit, West Siberia. A discovery gas capacity, 1.7×10^{14} mol, corresponds to the total rock volume of the this field $\approx 130 \text{ km}^3$, taking the initial total gas pressure, $P_{\text{TOTAL}} = 122 \text{ atm}$, the average temperature, 310 K, and the average porosity of the gas bearing rocks, $\phi = 0.27$. The average concentration of $^{40}\text{Ar}_{\text{AIR}} = 55 \times 10^{-6}$ in gases from this field (Prasolov, 1990) gives the total amount of $^{40}\text{Ar}_{\text{AIR}} = 9.3 \times 10^9$ mol. Comparing this value with the ASW concentration of argon in sea water, $^{40}\text{Ar}_{\text{ASW}} = 1.0 \times 10^{-2} \text{ mol m}^{-3}$ gives the water volume required to supply the $^{40}\text{Ar}_{\text{AIR}}$ in the Cenomanian field, $V_{\text{W}} \approx 900 \text{ km}^3$, far in excess of the *in-situ* field volume. This estimate is a minimum as it assumes complete partitioning of $^{40}\text{Ar}_{\text{AIR}}$ from ground water into the gas phase.

A similar estimate can be derived from the $^4\text{He}^*$ inventory in the gas and water phases. The $^4\text{He}^*$ content, 1.4×10^{-4} , and the field capacity give the total amount of $^4\text{He}^* = 2.4 \times 10^{10}$ mol. Assuming that: (i) the field has been formed relatively recently and the $^4\text{He}^*$ was generated in sedimentary rocks and accumulated in the ground waters since 100 Ma ago (the Cenomanian age); (ii) concentrations [$\mu\text{g g}^{-1}$] of U = 2.5, Th = 6.9, proposed for an “average” sedimentary rock of West Siberia by Prasolov (1990); (iii) an average porosity of water bearing rocks $\phi = 0.1$, then Eqn (1) gives $^4\text{He}^*_{\text{PW}} = 5.4 \times 10^{-2} \text{ mol m}^{-3}$. Correspondingly, $\approx 440 \text{ km}^3$ of ground water is required to supply the Cenomanian field with radiogenic $^4\text{He}^*$.

The two estimates of the ground water volume, 900 and 440 km^3 , derived from $^{40}\text{Ar}_{\text{AIR}}$ and U-Th- $^4\text{He}^*$ systematics, respectively, may be considered as being in reasonable agreement, taking into account several poorly determined parameters involved in these estimates. The volume of water-bearing rock (with the same porosity as above, 0.1) required to supply the noble gases in the Cenomanian field, *i.e.*, $V_{\text{WBR}} \approx (900 + 440)/(2 \times 0.1) \approx 6700 \text{ km}^3$, exceeds the Urengoi trap rock volume by a factor of ≈ 50 .

Ballentine et al. (1991) used noble gases to constrain the scale of the processes, involved in formation of the Hajduszoboszlo and Ebes hydrocarbon gas fields in the Pannonian basin, Hungary (total gas capacity 1.5×10^{12} ; reservoir volume $\approx 1.5 \text{ km}^3$). Comparison of the total amounts of air-derived $^{20}\text{Ne}_{\text{AIR}} (\approx 3.1 \times 10^5 \text{ mol})$ in this field and the ASW concentration of ^{20}Ne in sea water ($\approx 6.70 \times 10^{-12} \text{ mol ml}^{-1}$) gives the volume of rocks (with 10% porosity) $\approx 470 \text{ km}^3$, from which all Ne dissolved

in pore water should be partition into the gas phase. Regarding radiogenic isotopes, assuming the maximum time of their accumulation in rocks with average crustal concentrations of U and Th to be equal to the age of the Pannonian basin, 20 Ma, then Eqn. (1a) gives ${}^4\text{He}^* = 1.34 \times 10^{-9} \text{ mol cm}^{-3}$. Taking into account the total amount of ${}^4\text{He}^*$ in the gas field, $\approx 8.9 \times 10^8 \text{ mol}$, then the volume of rocks, from which all generated He should partition into the gas phase, is equal to $\approx 670 \text{ km}^3$, similar to that calculated from ASW Ne. The volume of the water-bearing rock required to account for the ASW noble gases in the reservoir exceeds the size of the gas reservoir rock volume by a factor of $V_{\text{WBR}} / V_{\text{HBR}} \approx 450$. A close similarity of observed $\text{CH}_4 / {}^{40}\text{Ar}_{\text{AIR}}$ ratio and that predicted from the solubility equilibrium is consistent with a model envisaging gas transfer by CH_4 - saturated ground water following by gas separation due to water cooling or decompression.

5.2. Excess radiogenic noble gases in hydrocarbon field: flux from deep crust

In this section we compare the noble gas characteristics of “average” gas fields (Section 3) with those highly enriched in radiogenic species. Hiyagon and Kennedy (1992) reported rather variable contributions of radiogenic noble gas isotopes within Cretaceous and Devonian reservoirs in the Alberta Basin, Canada. In some samples, group A, enhanced ${}^3\text{He} / {}^4\text{He}$ ratios were observed, probably indicating some contribution of mantle He to the hydrocarbon reservoirs, while other samples, group B, were highly enriched in radiogenic isotopes. In group B the ratios of $f {}^4\text{He} / {}^{20}\text{Ne}$, ${}^{21}\text{Ne} / {}^{22}\text{Ne}$ and ${}^{40}\text{Ar} / {}^{36}\text{Ar}$ approach 1.4×10^5 , 0.08 and 6500, respectively, corresponding to rather long apparent recharge – partition time intervals. Using the first ratio with parameters, shown in Footnote “c” to Table 1, gives apparent RPTI $\approx 1600 \text{ Ma}$, whereas the last ratio corresponds to $>1400 \text{ Ma}$, both values substantially exceeding the stratigraphic ages of reservoir rocks (below 400 Ma). This discrepancy indicates a contribution of radiogenic isotopes from external sources. Taking into account that the He partial pressure in hydrocarbon field increases with decreasing distance between the field site and the basement surface (Fig. 7) the authors consider the flux from the basement to be responsible for the high abundances of radiogenic species in the Alberta. The inferred flux of ${}^4\text{He}^*$ in selected reservoirs of the Alberta Basin approaches $\approx 6.6 \times 10^{-7} \text{ mol m}^{-2} \text{ a}^{-1}$, somewhat below the average crustal flux $\approx 1.5 \times 10^{-6} \text{ mol m}^{-2} \text{ a}^{-1}$ (e.g., O’Nions and Oxburgh, 1988; Hiyagon and Kennedy, 1992). Pinti and Marty (1995) studied noble gas isotope abundances in crude oils from Paris Basin (France) and also concluded that the radiogenic isotopes were transferred into Keuper reservoirs from the underlying basement.

Fig. 7.

Concentrations of air-derived Ar and Kr in the Alberta sedimentary basin correspond to the G / W ratios which range from 2 to 20, in overall agreement with those obtained for other hydrocarbon fields (Fig. 1). Also, air Xe has probably been transferred underground via sorption.

5.3. Sources of highly radiogenic noble gases in Brazil hydrocarbon fields: in situ accumulation versus partitioning from ancient ground waters

Rather high concentrations of ${}^4\text{He}^*$, ${}^{21}\text{Ne}^*$, ${}^{22}\text{Ne}^*$, ${}^{40}\text{Ar}^*$ and high ${}^4\text{He}^* / {}^{20}\text{Ne}_{\text{ASW}}$, ${}^{21}\text{Ne}^* / {}^{21}\text{Ne}_{\text{ASW}}$, ${}^{22}\text{Ne}^* / {}^{22}\text{Ne}_{\text{ASW}}$, ${}^{40}\text{Ar}^* / {}^{40}\text{Ar}_{\text{ASW}}$ ratios were reported for hydrocarbon reservoirs in the Brazilian sedimentary basin (Prinzhofer and Battani, 2003). To explain these observations (seen in Fig. 8), the authors proposed that “The good consistency between values of slope ratios confirms the quantitative estimate of the relative residence time of hydrocarbons in these reservoirs, the

hydrocarbons of reservoirs C and D having a residence time approximately 35% longer than in the reservoirs A and B”, the trap rock ages of these reservoirs being younger than Cambrian (Milani and Zalan, 1999).

To comment on this interpretation, we performed an additional “quantitative estimate” of residence times of the hydrocarbon gases. $^4\text{He}^*$ concentration in the gas samples varies from 0.0027 to 0.001 (see Fig. 11 in Prinzhofer and Battani, 2003). Assuming an average depth of the hydrocarbon fields of ≈ 2000 m, a temperature of 70°C , a porosity of 20 % (e.g., Milani and Zalan, 1999), then maximum and minimum $^4\text{He}^*$ concentrations in the host rocks are 3.8×10^{-6} and 1.4×10^{-6} mol cm^{-3} , respectively. Substitution of these concentrations along with the average crustal U and Th in Eqn. 1b gives meaningless $^4\text{He}^*$ accumulation time intervals, 7.6 and 6.3 Ga, respectively. Similar enormously long time scales follow from $^{21}\text{Ne}^*$ and $^{40}\text{Ar}^*$ concentrations seen in Fig. 8; for example 7.6 Ga is required to generate $^{21}\text{Ne}^* = 1 \times 10^{-10}$ in a gas reservoir with the same parameters. These estimates indicate that reasonable accumulation time intervals can’t be obtained by varying the field parameters assumed above as well as that it is not possible to explain the different concentrations of radiogenic noble gas species by *in situ* accumulation, in contrast to the proposal by Prinzhofer and Battani (2003).

Fig. 8.

Rejecting the *in situ* accumulation hypothesis, we suggest the “general” scenario discussed in Section 3: in the course of hydrocarbon field formation hydrocarbon phases contacted with more ancient (fields C,D) and less ancient (A,B) ground waters. Assuming ASW concentrations of air-derived species for sea water, other parameters from the Footnotes to Table 1 and a 5 % porosity of water bearing layers, the recharge – hydrocarbon production interval, corresponding to the radiogenic/air-derived isotope ratios ($^4\text{He}^*/^{20}\text{Ne}_{\text{ASW}} \approx 1 \times 10^5$; $^{21}\text{Ne}^*/^{21}\text{Ne}_{\text{ASW}} \approx 1$; $^{40}\text{Ar}^*/^{40}\text{Ar}_{\text{ASW}} \approx 5$ (see Fig 7 and Prinzhofer and Battani, 2003), amounts to ≈ 450 Ma for U-Th- $^4\text{He}^*$ - $^{21}\text{Ne}^*$ and > 320 Ma for K-Ar* systematics. This time interval is comparable with the stratigraphic ages of Ordovician-Devonian Sequence in the Amazonian Basin (Fig. 4). The low porosity can result from large depths of the Amazonian sediments, down to 6 km (Milani and Zalan, 1999). The correlations seen in Figure 7ab could reflect variable mixing between hydrocarbons and noble gases in the course of field formation or/and from variable losses of noble gases (postulated by Prinzhofer and Battani, 2003).

Summarizing, even though certain parameters, used for the noble-gas-derived time scales, are generally poorly known, the above examples show that the respective estimates are useful for better understanding of formation and evolution of hydrocarbon accumulations.

6. Hydrocarbons with small contribution of radiogenic noble gas isotopes

The lowest concentrations of radiogenic noble gases isotopes are typical of young hydrocarbon manifestations and low-capacity fields, situated in active tectonic settings. Island arcs belong to such settings and as an example we present data obtained for gases collected from boreholes (200 to 1200 m deep) and methane seepages in the Green Tuff province and in Kanto district, Honshu Island, Japan (Sano et al., 1982; Wakita et al., 1990). From data available in the noble gas data base (Polyak et al., 2015) we selected samples with ($^{20}\text{Ne}/^{40}\text{Ar}$) ratios varying between AIR and ASW values, thus indicating a small noble gases fractionation during underground noble gases transfer. In this case the assumption that $(^4\text{He}^*/^{20}\text{Ne})_{\text{PORE WATER}} \approx (^4\text{He}^*/^{20}\text{Ne})_{\text{GAS PHASE}}$ appears to be correct. These samples show variable concentrations of air-derived noble gases, $[^{20}\text{Ne}]_{\text{AIR}}$ varies from 1.4×10^{-7} to 2.4×10^{-6} , whereas the $^4\text{He}^*/^{20}\text{Ne}_{\text{AIR}}$ ratio is less variable, within a factor of ≈ 2 . The simplest explanation of

these observation implies mixing of air and radiogenic noble gases in the course of ground water migration following by their different dilution by methane.

Assuming $(^4\text{He}/^{20}\text{Ne})_{\text{AIR}}$ in methane to be equal to the ASW value (0.254) and correcting a minimum measured ratio (1.78) for the contribution of air-derived $^4\text{He}_{\text{AIR}}$, we obtain $^4\text{He}^*/^{20}\text{Ne}_{\text{AIR}} \approx 1.5$. Substituting this value in Eqn. 2 gives a recharge –partition interval as short as ≈ 18 Ka. Several other samples show similar ratios of $^4\text{He}^*/^{20}\text{Ne}_{\text{AIR}} (\leq 4)$ and thus similar recharge – partition time intervals, which are orders of magnitude younger than the stratigraphic ages of organic-bearing shale (within 16 to 10 Ma age interval) and hydrocarbon trap rocks (older than ≈ 5 Ma).

Even though the time interval obtained above, ≈ 20 Kyr, includes groundwater migration time as well as time of methane generation and uplift, this interval is so short that it may be used to estimate the lower limit of the rate of hydrocarbon generation. Multiplying the $^4\text{He}^*$ production rate in a present day rock (having average upper-crust U and Th concentrations), $2.8 \times 10^{-17} \text{ mol g}^{-1} \text{ a}^{-1}$, by the highest $\text{CH}_4 / ^4\text{He}^*$ ratio ($\approx 2 \times 10^6$) observed in gas emanating from the surface of the Chonan gas field, Kanto district, gives the CH_4 production rate at $5.4 \times 10^{-11} \text{ mol g}^{-1} \text{ a}^{-1}$. Interestingly, this value is similar to the independent estimates for sediments from the Caspian depression and sea sediments (Neruchev et al., 1998, Tables 5.5, 5.7). If some part of the above time interval could be constrained from *a priori* data, for example from the rate of ground water flow in a given environment, the hydrocarbon formation rate can be determined more precisely by this “noble gas approach”.

A similar approach can be used with respect to other hydrocarbon manifestations, such as mud volcanoes, sometimes also showing quite high $\text{CH}_4 / ^4\text{He}^*$ ratios $\approx 10^5$ (e.g., Baciu et al., 2007).

7. Concluding remarks

More than five decades ago the pioneering paper by Zartman, Wasserburg and Reynolds (1961) opened the modern noble gas isotope geochemistry. Since then this branch of Earth Sciences has seen remarkable progress, from study of sources and the origin and evolution of noble gases themselves (Ozima and Podosek, 1983; Mamyrin and Tolstikhin, 1984) to applying the knowledge obtained to a wide variety of geochemical problems (Porcelli, Ballentine and Wieler, eds, 2002; Burnard, 2013), including those related to the origin of hydrocarbon materials, their fluxes from different sources, formation and evolution of the hydrocarbons.

Even a short list of problems of terrestrial hydrocarbons, to which noble gases tracers are being applied, appears to be quite impressive:

- Using noble gas isotopes to understand sources of hydrocarbons and constrain processes of their generation.
- Using noble gases to model partitioning among gas, oil and water phases.
- Quantitative estimates of gas / water / oil ratios using air-derived noble gas species.

Quantitative estimates of ratios of water-bearing over hydrocarbon trap rocks using both air-derived and radiogenic noble gas isotopes.

Using a large available data base on noble gas isotopes in hydrocarbon fields allows an important conclusion to be derived on time scales of accumulation of hydrocarbon fields: ages of the ground waters, participating in hydrocarbon formation, and the hydrocarbon source and trap lithologies are similar. This is typical for hydrocarbon fields in different tectonic environments. This also means that hydrocarbon fields were formed relatively recently, generally they are much younger than the hydrocarbon trap structures. The dependence of time bearing isotope ratios, such as $^4\text{He}^*/^{20}\text{Ne}_{\text{ASW}}$, $^{21}\text{Ne}^*/^{21}\text{Ne}_{\text{ASW}}$, $^{40}\text{Ar}^*/^{40}\text{Ar}_{\text{ASW}}$, on tectonic environment also indicates that local processes are generally responsible for accumulation of radiogenic noble gas isotopes in ancient ground waters, presently observed in hydrocarbon accumulations. Fluxes of radiogenic noble gas species from

external sources should be considered as exceptions; these fluxes are revealed by the long recharge – partition time intervals, greatly exceeding the stratigraphic ages of the hydrocarbon source rocks.

The translation of the radiogenic / air-derived noble gas ratios into apparent time scales bridges the noble gas data with geological environments. Even though the time scales, obtained by such approach, are not precise at present, we would like to emphasize that the studies of noble gas isotope inventories in fluid phases and in rocks hosting these phases, is a promising way to make better estimates. Studies of rock-water systems are still very narrow. The authors of fluid-related papers generally ignore studies of associated solids (rocks, minerals), typically considering that they know about solids well enough from hypothetical “average” data. Meanwhile rare contributions, in which attention was paid to both mineral and fluid reservoirs, indeed show the validity of both rock- and water- studies.

Another poorly investigated problem relates to “fossil” pore waters with small concentrations of highly fractionated noble gases, retained after their partitioning between the water and hydrocarbon phase(s). Gases released from such waters and avoided mixing with ASW waters are also interesting rarely observed samples, able to shed light on post fractionation evolution of crustal fluids.

Acknowledgements

All the authors thank the Sloan Foundation, Deep Earth Energy directorate and personally David Cole, Isabelle Daniel and Edward Young for support of this project during four years (project numbers 60033365 and 60040915); without this support the noble gas data base and this contribution could hardly be prepared. Our readers find most data used here in Polyak et al. (2015), also useful are references included in the data base.

The authors very much appreciate careful constructive reviews of the early version of the manuscript by Yuri Taran, Alain Prinzhofer and Igor Villa and we thank all these colleagues. The paper was improved due to careful and constructive review by Daniele Pinti. We also thank Margaret Vetrin for preparing the figures and references to this contribution and Oliver Warr for his long-term help with the literature.

References

- Aeschbach-Hertig, W., El-Gamal, H., Wieser, M., Palcsu, L., 2008. Modeling excess air and degassing in groundwater by equilibrium partitioning with a gas phase. *Water Resour. Res.* 44, W08449, doi:10.1029/2007WR006454.
- Baciu, C., Caracausi, A., Etiope, G., Italiano, F., 2007. Mud volcanoes and methane seeps in Romania: main features and gas flux. *Annals of Geophysics* 50, 501–511.
- Ballentine, C. J., O’Nions, R. K., 1992. The nature of mantle neon contributions to Vienna Basin hydrocarbon reservoirs. *Earth Planet. Sci. Lett.* 113, 553–567.
- Ballentine, C. J., O’Nions, R. K., 1994. The use of natural He, Ne and Ar isotopes to study hydrocarbon-related fluid provenance, migration and mass balance in sedimentary basins, in: Parnell, J. (Ed.), *Geofluids: Origin, migration and evolution of fluids in sedimentary basins*. Geological Society, Special Publication 78, pp. 347–361.
- Ballentine, C.J. and Hall, C.M. 1999. Determining paleotemperature and other variables by using an error-weighted, nonlinear inversion of noble gas concentrations in water. *Geochim. Cosmochim. Acta* 63, 2315–2336.
- Ballentine, C. J., Sherwood Lollar, B., 2002. Regional groundwater focusing of nitrogen and noble gases into the Hugoton-Panhandle giant gas field, USA. *Geochim. Cosmochim. Acta* 66, 2483–2497.
- Ballentine, C. J., O’Nions, R. K., Oxburgh, E. R., Horvath, F., Deak, J., 1991. Rare-gas constraints on hydrocarbon accumulation, crustal degassing and groundwater flow in the Pannonian Basin. *Earth Planet. Sci. Lett.* 105, 229–246.
- Ballentine, C. J., O’Nions, R. K., Coleman, M. L., 1996. A Magnus opus: Helium, neon, and argon isotopes in a North Sea oilfield. *Geochim. Cosmochim. Acta* 60, 831–849.
- Barry, P. H., Lawson, M., Meurer, W. P., Warr, O., Mabry, J. C., Byrne, D. J., Ballentine, C. J., 2016. Noble gases solubility models of hydrocarbon charge mechanism in the Sleipner Vest gas field. *Geochim. Cosmochim. Acta* 194, 291–309.
- Baxter, E. F., 2003. Quantification of the factors controlling the presence of excess ^{40}Ar or ^4He . *Earth Planet. Sci. Lett.* 216, 619–634.
- Bosch, A., Mazar, E., 1988. Natural gas association with water and oil as depicted by atmospheric noble gases: case studies from the southeastern Mediterranean Coastal Plain. *Earth Planet. Sci. Lett.* 87, 338–346.
- Burnard, P. E. (Ed.), 2013. *The Noble Gases as Geochemical Tracers*. Springer, Heidelberg, 391 pp.
- Dai, J., Zou, C., Zhang, S., Li, J., Ni, Y., Hu, G., Luo, X., Tao, S., Zhu, G., Mi, J., Li, Z., Hu, A., Yang, C., Zhou, Q., Shuai, Y., Zhang, Y., Ma, C., 2008. Discrimination of abiogenic and biogenic alkane gases. *Science in China, Series D: Earth Sciences* 51, 1737–1749.
- Elliot, T., Ballentine, C. J., O’Nions, R. K., Ricchiuto, T., 1993. Carbon, helium, neon and argon isotopes in a Po Basin (northern Italy) natural gas field. *Chemical Geology* 106, 429–440.
- Etiope, G., Lassey, K. R., Klusman, R. W., Baschi, E., 2008. Reappraisal of the fossil methane budget and related emission from geologic sources. *Geophys. Res. Lett.* 35, L09307, doi:10.1029/2008GL033623.
- Gavrilov, E. Ya., Teplinskiy, G. I., 1973. Distribution of argon isotopes in hydrocarbon gases. *Geokhimiya* 4, 559–569 (in Russian).
- Gavrilov, E. Ya., Zhurov, Yu. A., Teplinskiy, G. I., 1972. On the relationship of the isotope composition of argon and carbon in natural gases. *Doklady of the USSR Academy of Sciences* 206, no. 2, 448–451 (in Russian).

- Gerling, E. K., Tolstikhin, I. N., Shukolyukov, Yu. A., 1967. Argon and helium isotopes in natural hydrocarbon gases. *Geokhimiya* 5, 608–617 (in Russian).
- Gilfillan, S. M. V., Ballentine, C. J., Holland, G., Blagburn, D., Sherwood Lollar, B., Stevens, S., Schoell, M., Cassidy, M., 2008. The noble gas geochemistry of natural CO₂ gas reservoirs from the Colorado Plateau and Rocky Mountain provinces, USA. *Geochim. Cosmochim. Acta* 74, 1174–1198.
- Gilfillan, S. M. V., Wilkinson, M., Haszeldinea, R. S., Shiptonb, Z. K., Nelsonc, S. T., Poreda, R. J., 2011. He and Ne as tracers of natural CO₂ migration up a fault from a deep reservoir. *Intern. J. Greenhouse Gas Control*. 5, 1507–1516.
- Hiyagon, H., Kennedy, B. M., 1992. Noble gases in CH₄-rich gas fields, Alberta, Canada. *Geochim. Cosmochim. Acta* 56, 1569–1589.
- Holland, G., Sherwood Lollar, B., Li, L., Lacrampe-Couloume, G., Slater, G. F., Ballentine, C. J., 2013. Deep fracture fluids isolated in the crust since the Precambrian era. *Nature* 497, 357–360.
- Jenden, P., Hilton, D., Kaplan, I., Craig, H., 1993. Abiogenic hydrocarbons and mantle helium in oil and gas fields, in: Howell, D. G. (Ed.), *The Future of Energy Gases*. U. S. Geological Survey Professional Paper 1570, pp. 31–56.
- Jenden, P. D., Kaplan, I. R., Poreda, R. J., Craig, H., 1988. Origin of nitrogen-rich natural gases in the California Great Valley: Evidence from helium, carbon and nitrogen isotope ratios. *Geochim. Cosmochim. Acta* 52, 851–861.
- Jin, Z., Zhang, L., Yang, L., Cui, Y., Milla, K., 2009. Using carbon, hydrogen and helium isotopes to unravel the origin of hydrocarbons in the Wujiaweizi area of the Songliao Basin, China. *Episodes* 32, no. 3, 167–176.
- Johnson, H., Leslie, A.B., Wilson, C.K., Andrews, I.J., Cooper, R.M., 2005. Middle Jurassic, Upper Jurassic and Lower Cretaceous of the UK Central and Norther North Sea. *British Geological Survey Research Report RR/03/001*, 42 pp.
- Kamenskiy, I. L., Prasolov, E. M., Tikhomirov, V. V., 1975. Isotope data on juvenile components in Sakhalin gas pools. *Geochemistry International* 11, no. 4, 845–849.
- Klemme, H.D., Ulmishek G.F., 1991. Effective petroleum source rocks of the world: Stratigraphic distribution and controlling depositional factors. *Amer. Ass. Petrol. Geo. Bull.* 75, 1809–1851.
- Lehmann, B. E., Love, A., Purtschert, R., Collon, P., Loosli, H. H., Kutschera, W., Beyerle, U., Aeschbach-Hertig, W., Kipfer, R., Frape, S. K., Herczeg, A., Moran, J., Tolstikhin, I. N., Groning, M., 2003. A comparison of groundwater dating with ⁸¹Kr-, ³⁶Cl- and ⁴He in four wells of the Great Artesian Basin, Australia. *Earth Planet. Sci. Lett.* 211, 237–250.
- Lobkov, V. A., Prasolov, E. M., 1976. Carbon and argon isotopes in gases of the Lena-Viluy syncline. *Doklady of the USSR Academy of Sciences* 228, no. 1, 202–204 (in Russian).
- Love, A. J., Herczeg, A. L., Sampson, L., Cresswell, R. G., Fifield, L. K., 2000. Sources of chloride and implications for ³⁶Cl dating of old groundwater, southwestern Great Artesian Basin, Australia. *Water Resour. Res.* 36, 1561–1574.
- Ma, L., Castro, M. C., Hall, C. M., Walter, L. M., 2005. Cross-formational flow and salinity sources inferred from a combined study of helium concentrations, isotopic ratios, and major elements in the Marshall aquifer, southern Michigan. *Geochem. Geophys. Geosys.* 6, Q10004, doi:10.1029/2005GC001010.
- Magoon, L. B., Dow, W. G., 1994. The petroleum system, in: Magoon, L. B., Dow, W. G. (Eds.), *The Petroleum system—From source to trap*. American Association of Petroleum Geologists Memoir. 60, pp. 3–24.
- Mamyrin, B. A., Tolstikhin, I. N., 1984. Helium isotopes in nature. *Developments in Geochemistry*. Elsevier Sci. Pub., Amsterdam, 273 pp.

- Marine, I. W., 1979. The use of naturally occurring helium to estimate groundwater velocities for studies of geologic storage of radioactive waste. *Water Resour. Res.* 15, 1130–1136.
- Marty, B., 1995. Rare gas measurements in fluids from the Pannonian basin, Hungary. CRPG/ENSG Report. Nancy, France.
- Milani, E. J., Zalan, V., 1999. An outline of the geology and petroleum systems of the Paleozoic interior basins of South America. *Episodes* 22, 199–205.
- Nagao, K., Takaoka, N., Matsubayashi, O., 1981. Rare gas isotopic compositions in natural gases of Japan. *Earth Planet. Sci. Lett.* 53, 175–188.
- Neruchev, S. G., Rogozina, T. A., Shimanski, V. K., 1998. Handbook on gas and oil geochemistry. Nedra, St. Petersburg, 575 pp. (In Russian).
- Nesmelova, Z. N., Kamenskii, I. L., Lobkov, V. A., 1975. Geochemical study of gas and gas condensate deposits in the Western Ciscaucasia according to the isotope composition of carbon, argon, helium. *Proceedings of VNIGNI* 174, pp. 106–111 (in Russian).
- Nesterov, I. I., Nemchenko, I. I., Rovenskaya, A. S., Shpilman, A. K., 1976. Isotopic composition of argon of natural gases of the North of Western Siberia in connection with their genesis. *Doklady of the USSR Academy of Sciences* 230, no. 4, 942–944 (in Russian).
- Ni, Y., Dai, J., Tao, S., Wu, X., Liao, F., Wu, W., Zhang, D., 2014. Helium signatures of gases from the Sichuan Basin, China. *Organic Geochemistry* 74, 33–43.
- O’Nions, R. K., Oxburgh, E. R., 1988. Helium, volatile fluxes, and the development of continental crust. *Earth Planet. Sci. Lett.* 90, 331–347.
- Ozima, S., Podosek, F. A., 1983. Noble gas geochemistry. Cambridge University Press, Cambridge, U. K., 367 pp.
- Pearson, F. J., Balderer, W., Loosli, H. H., Lehmann, B. E., Matter, A., Peters, T., Schmassmann, H., and Gautschi, A., 1991. Applied isotope hydrogeology: A case study in Northern Switzerland. Elsevier Sci. Pub., Amsterdam, 439 pp.
- Peeters, F., Beyerle, U., Aeschbach-Hertig, W., Holocher, J., Brennwald, M. S., Kipfer, R., 2002. Improving noble gas based paleoclimate reconstruction and groundwater dating using $^{20}\text{Ne}/^{22}\text{Ne}$ ratios. *Geochim. Cosmochim. Acta* 67, 587–600.
- Pinti, D. L., Marty, B., 1995. Noble gases in crude oils from Paris Basin, France: Implications for the origin of fluids and constraints on oil-water-gas interactions. *Geochim. Cosmochim. Acta* 59, 3389–3404.
- Pinti, D. L., Marty, B., 2000. Noble gases in oil and gas fields: origins and processes, in: Kyser, K. (Ed.), *Fluids and Basin Evolution. Miner. Ass. Canada Short Course*. 28, pp. 160–196.
- Pollastro, R. M., 2003. Total petroleum systems of the Paleozoic and Jurassic, Greater Ghawar Uplift and adjoining provinces of Central Saudi Arabia and Northern Arabian Gulf. *U.S. Geol. Survey Bull.* 2202-H, 100 pp.
- Polyak, B. G., Prasolov, E. M., Tolstikhin, I. N., Yakovlev, L.E., Ioffe, A.I., Kikvadze, O.E., Vereina, O.B., Vetrina, M.A., 2015. Noble Gas Isotope Data Base.
<<http://data.deepcarbon.net/ckan/dataset/523f4bf3-5de4-4c30-9c62-34af0dc62f70>>
- Porcelli, D., Ballentine, C. J., Wieler, R. (Eds.), 2002. Noble gases in geochemistry and cosmochemistry. Mineral. Soc. Amer., Washington, 845 pp.
- Prasolov, E. M., 1981. Peculiarities of gas formation and gas accumulation in the light of isotopic data, in: *Origin and composition of natural gases as recorded by isotope geochemistry data. Proceedings of VNIGRI, Leningrad*, pp. 4–22 (in Russian).
- Prasolov, E. M., 1990. The isotope geochemistry and origin of natural gases. Nedra, Leningrad, 283 pp. (In Russian).

- Prasolov, E. M., Lobkov, V. A., Yakutseni, V. P., 1980. The intensity and depth generation of methane in the Earth's crust (by isotopic data). *Doklady of the USSR Academy of Sciences* 252, no. 6, 1476–1479 (in Russian).
- Prasolov, E. M., Kamenskii, I. L., Meshik, A. P., 1981. On the formation of gas fields in the North of Western Siberia from isotope data, in: *Origin and formation of the composition of natural gases on the base of isotope geochemistry data*. Proceedings of VNIGRI, Leningrad, pp. 64–82 (in Russian).
- Prasolov, E. M., Travnikova, L. G., Verkhovsky, A. B., and others, 1987. Isotopic composition of gases of the salt-bearing sediments. Nitrogen and carbon. *Geokhimiya* 4, 525–532 (in Russian).
- Prinzhofer, A., 2013. Noble gas in gas and oil accumulations, in: *Burnard, P. (Ed.), The noble gases as geochemical tracers*. Springer, Heidelberg, pp. 225–247.
- Prinzhofer, A., Battani, A., 2003. Gas Isotopes Tracing: an Important Tool for Hydrocarbons Exploration. *Oil & Gas Science and Technology - Rev. IFP*. 58, 299–311.
- Prinzhofer, A., Neto, E. V. D., Battani, A., 2010. Coupled use of carbon isotopes and noble gas isotopes in the Potiguar basin (Brazil): Fluids migration and mantle influence. *Marine and Petroleum Geology* 27, 1273–1284.
- Rudnick, R. L., Gao S., 2003. Composition of the Continental Crust, in: *Rudnick R. L. (Ed.), The Crust*. Elsevier-Pergamon, Oxford.
- Sano, Y., Tominaga, T., Nakamura, Y., Wakita, H., 1982. $^3\text{He}/^4\text{He}$ ratios of methane-rich natural gases in Japan. *Geochem. J.* 16, 237–245.
- Sathaye, K. J., Larson, T. E., Hesse, M. A., 2016. Noble gas fractionation during subsurface gas migration. *Earth Plan. Sci. Lett.* 450, 1–9.
- Smith, S. P., Kennedy, B. M., 1983. The solubility of noble gases in water and in NaCl brine. *Geochim. Cosmochim. Acta* 47, 503–515.
- Solomon, D. K., 1996. Source of radiogenic helium-4 in shallow aquifers: Implications for dating young groundwater. *Water Res. Res.* 32, 1805–1813.
- Tolstikhin, I. N., 1985. Isotope geochemistry of helium, argon and rare gases. Nauka, Leningrad, 200 pp. (In Russian).
- Tolstikhin, I. N., Lehmann, B. E., Loosli, H. H., Gautschi, A., 1996. Helium and argon isotopes in rocks, minerals and related ground waters: A case study in Northern Switzerland. *Geochim. Cosmochim. Acta* 60, 1497–1514.
- Tolstikhin, I., Waber, H. N., Kamensky, I., Loosli, H. H., Skiba, V., Gannibal, M., 2011. Production, redistribution and loss of helium and argon isotopes in a thick sedimentary aquitard-aquifer system (Molasse Basin, Switzerland). *Chemical Geology* 286, 48–58.
- Torgersen, T., Ivey, G. N., 1985. Helium accumulation in groundwater. II: A model for the accumulation of the crustal ^4He degassing flux. *Geochim. Cosmochim. Acta* 49, 2445–2452.
- Torgersen, T., Kennedy, B. M., 1999. Air-Xe enrichments in Elk Hills oil field gases: role of water in migration and storage. *Earth Planet. Sci. Lett.* 167, 239–253.
- Voronov, A. N., Prasolov, E. M., 1974. Radiogenic argon in gas fields of the North-Eastern part of the Volga-Ural oil-gas zone. *Geokhimiya* 11, 1700–1710 (in Russian).
- Voronov, A. N., Prasolov, E. M., Tikhomirov, V. V., 1974. Ratios of radiogenic argon and helium isotopes in gas fields. *Geokhimiya* 12, 1842–1955 (in Russian).
- Verchovsky, A.B., Markov, V.M., Prasolov, E.M., Shukolyukov, Yu.A., 1988. Atmospheric noble gas abundances in gas fields. *Doklady of the USSR Academy of Sciences* 303, 1473–1477 (in Russian).
- Wakita, H., Sano, Y., Urabe, A., Nakamura, Y., 1990. Origin of methane-rich natural gas in Japan: formation of gas fields due to large-scale submarine volcanism. *Appl. Geochem.* 5, 263–268.

- Weiss, R. F., 1970. The solubility of nitrogen, oxygen and argon in water and seawater. *Deep-Sea Res.* 17, 721–735.
- Welhan, J. A., Craig, H., 1983. Methane, hydrogen and helium in hydrothermal fluids at 21 °N on the East Pacific Rise, in: Rona, P. A. et al. (Eds.), *Hydrothermal Process at Seafloor Spreading Centers*. NATO Conf., Plenum Press, New York, pp. 391–409.
- Xu, Y. C., Wang, X. B., Wu, R. M., 1982. Rare gas isotopic composition of natural gases. *Geochemistry (China)* 1, no 2, 218–232.
- Xu, S., Nakai, S., Wakita H., 1995a. Helium isotope compositions in sedimentary basins in China. *Applied Geochemistry* 10, 643–656.
- Xu, S., Nakai, S., Wakita, H., Wang, X., 1995b. Mantle-derived noble gases from Songliao Basin, China. *Geoch. Cosmochim. Acta* 59, no. 22, 4675–4683.
- Zartman, R. E., Wasserburg, G. J., Reynolds, J. H., 1961. Helium, argon and carbon in some natural gases. *J. Geophys. Res.* 66, 277–306.
- Zhou, Z., Ballentine, C. J., Kipfer, R., Schoell, M., Thibodeaux, S., 2005. Noble gas tracing of groundwater/coaled methane interaction in the San Juan Basin, USA. *Geochim. Cosmochim. Acta* 69, 5413–5428.
- Zhou, Z., Ballentine, C. J., Schoell, M., Stevens, S. H., 2012. Identifying and quantifying natural CO₂ sequestration processes over geological timescales: The Jackson Dome CO₂ Deposit, USA. *Geochim. Cosmochim. Acta* 86, 257–275.

Figure Captions

Fig. 1. Gas / Water ratios [m^3 / m^3 , STP conditions] derived from Ar and Kr concentrations in natural gases from different gas accumulations.

The grey line shows equal G / W volume ratios for the two gases implying their equilibrium partitioning between gas and water phases. The array of the data points (127) defines the median ratio of $G / W \approx 6$ shown as a dotted line (64 samples to the right-top off this line and 63 samples to the left-bottom). $^{40}\text{Ar}_{\text{AIR}}$ concentrations presented in Table 1 give somewhat higher G / W ratios: 10, 14 and 17 for the ancient plates, young plates and mobile belts, respectively. Note that under “field” conditions the G / W ratios are much (by a factor ≈ 100) lower. Data from Bosch and Mazor (1988), Hiyagon and Kennedy (1992), Prinzhofer (2013).

Fig. 2. ^4He amounts in water- and gas- bearing rocks shown as a function of depth.

He amounts in gas (mainly hydrocarbon) bearing rocks were calculated using the He concentrations in gas samples and the depths of the boreholes, assuming the rock porosity to be 10 %. Gas temperatures and pressures (if not available in the sources of the data) were calculated assuming a geothermic gradient $0.03\text{ }^\circ\text{C m}^{-1}$ and hydrostatic pressure in the boreholes. N_2 , CO_2 and CH_4 define samples in which the contribution of a given component exceeds 50%; MIX means gas composition if the concentration of each component is less than 50%. Notice high ^4He in N-bearing gases. Taking into account: (i) an average time-integrated production ratio of $^4\text{He}^* / ^{40}\text{Ar}^* = 1.6$; (ii) almost complete transfer of $^{40}\text{Ar}^*$ from the solid earth into the atmosphere with $(^{40}\text{Ar}^* / \text{N}_2)_{\text{AIR}} = 0.012$, then the $^4\text{He} / \text{N}_2$ ratio in a “non-dissipating” atmosphere amounts to ≈ 0.02 . This ratio is expected to be higher in the present day average degassing flux because nitrogen was transferred into the atmosphere early in the earth history.

He amounts in water samples and in air-saturated water (dashed line) are those available in 0.1 ml water (or in 1 cm^3 of a rock with 10 % porosity). Note that He amounts in gas bearing rocks greatly exceed those in water bearing ones, up to a factor of ≈ 1000 . Data from the noble gas data base (Polyak et al., 2015).

Fig. 3. Correlation between $^4\text{He}^* / ^{40}\text{Ar}_{\text{AIR}}$ and $^{40}\text{Ar}^* / ^{40}\text{Ar}_{\text{AIR}}$ ratios in hydrocarbon accumulations and the recharge – partition intervals, derived from these ratios.

Grey solid and dashed lines show regression of the data and the present day crustal production $^4\text{He}^* / ^{40}\text{Ar}^*$ ratio, respectively. General parameters used for calculation of the recharge – partition intervals are presented in Footnotes to Table 1. Because of a better retention of $^{40}\text{Ar}^*$ compared with $^4\text{He}^*$, specific parameters related to this plot are: the $^{40}\text{Ar}^*$ loss coefficient $L_{40} = 0.5$; $^{40}\text{Ar}_{\text{ASW}}$ solubility for fresh water $10\text{ }^\circ\text{C}$.

This plot indicates: (i) loss of $^4\text{He}^*$ atoms from a parent rock into pore fluids is accompanying by $^{40}\text{Ar}^*$ loss; (ii) durations of the recharge – partition intervals appears to be those expected for sedimentary basins in different tectonic settings; (iii) an overall agreement between the two estimates.

Data are from the noble gas data base (Polyak et al., 2015) and from Prasolov (1990).

Fig. 4. Durations of the recharge – partition intervals (derived from $^4\text{He}^* / ^{40}\text{Ar}_{\text{ASW}}$ ratios) versus the average ages of hydrocarbon bearing rocks for different tectonic settings.

Equal values are shown by dashed line. Limits of the recharge – partition intervals correspond to Ar solubility in fresh $10\text{ }^\circ\text{C}$ water (top) and saline (sea) $40\text{ }^\circ\text{C}$ water (bottom; see Table 1, Footnotes to this Table and Eqn 2). Notice that the average durations of the recharge – partition intervals are

similar to the ages of hydrocarbon bearing lithologies; these relationships also envisage young ages for formation of hydrocarbon fields (see Text).

For comparison with the general trend the recharge-partition intervals for the Magnus oil field (the age of oil bearing lithology 150 Ma) are shown: 80 Ma (circle) obtained for $^4\text{He}^*/^{20}\text{Ne}_{\text{ASW}} = 7700$, 110 Ma (rhomb) for $^{21}\text{Ne}^*/^{21}\text{Ne}_{\text{ASW}} = 0.132$ and 100 Ma (cross) for $^{40}\text{Ar}^*/^{40}\text{Ar}_{\text{ASW}} = 0.48$ (U, Th, K concentrations and the above isotopic ratios are from Ballentine et al., 1996; other parameters from Footnotes to Table 1).

The interval, calculated using high ratios of $^{21}\text{Ne}^*/^{21}\text{Ne}_{\text{ASW}} \approx 1$ and $^{40}\text{Ar}^*/^{40}\text{Ar}_{\text{ASW}} \approx 5$ in hydrocarbons of the Amazonian basin, Brazil (shown as square in the right top corner, see also Fig. 8), can also be reconciled with the Devonian stratigraphic ages of sediments in this basin (see Text, Section 5). The arrow shows a rather long recharge – partition interval, ≈ 1500 Ma, derived from such ratios for the Alberta Basin, Canada, indication external flux of radiogenic species (see Text, Section 5.2, and Fig. 7).

Fig. 5. Comparison of the recharge – partition intervals (derived from $^4\text{He}^*/^{40}\text{Ar}_{\text{ASW}}$ ratios) for different tectonic settings (see Table 1 and Footnotes to this Table) versus the average ages of hydrocarbon source rocks.

See also Captions to Fig. 4. Modified after Klemme and Ulmishek (1991).

Fig. 6. $\text{CH}_4 / ^3\text{He}$ and $^4\text{He} / ^3\text{He}$ ratios in terrestrial gases, Russia.

The $\text{CH}_4 / ^3\text{He}$ vs. $^4\text{He} / ^3\text{He}$ coordinates allow two-component mixing to be interpolated by a straight line. Most continental hydrocarbon fields (rhombus) show radiogenic He isotope signature with negligible or only a small contribution of mantle He as indicated by data-points concentrated near the crustal production ratios “Crust (this work)”. CrustJ1993 is the crustal end member proposed by Jenden et al. (1993). An admixture of mantle He to the crustal methane + crustal helium gases is traced by the dashed line. A vertical trend with MORB-like $^4\text{He} / ^3\text{He}$ ratios (triangles) above or overlapping the mantle end member is defined by gas samples from tectonically active regions with small variable contributions of methane and variable contributions of mantle ^3He . Data points with only a small amount of variance from the air helium isotope ratio (circles) generally belong to relatively young ground water samples. Data are from the noble gas data base (Polyak et al., 2015).

Fig. 7. Correlation between partial pressure of radiogenic He in hydrocarbon fields of the Alberta sedimentary basin, Canada, and the depth interval between a field and the Precambrian crystalline basement.

Figure shows an exponential decrease of He concentration in a field with increasing distance from the basement. Samples from group B, highly enriched in radiogenic noble gas species, reside close to the surface of basement; therefore flux of fluids through faults in the basement is considered as a source of radiogenic isotopes in the Alberta Modified after Hiyagon and Kennedy(1992).

Fig. 8. Correlation between concentrations of radiogenic and air derived noble gas isotopes, $^{21}\text{Ne}^*$ vs. $^{21}\text{Ne}_{\text{AIR}}$ (a) and $^{40}\text{Ar}^*$ vs. $^{40}\text{Ar}_{\text{AIR}}$ (b), in the four hydrocarbon fields, the Amazonian hydrocarbon accumulations, Brazil. Modified after Prinzhofer and Battani (2003).

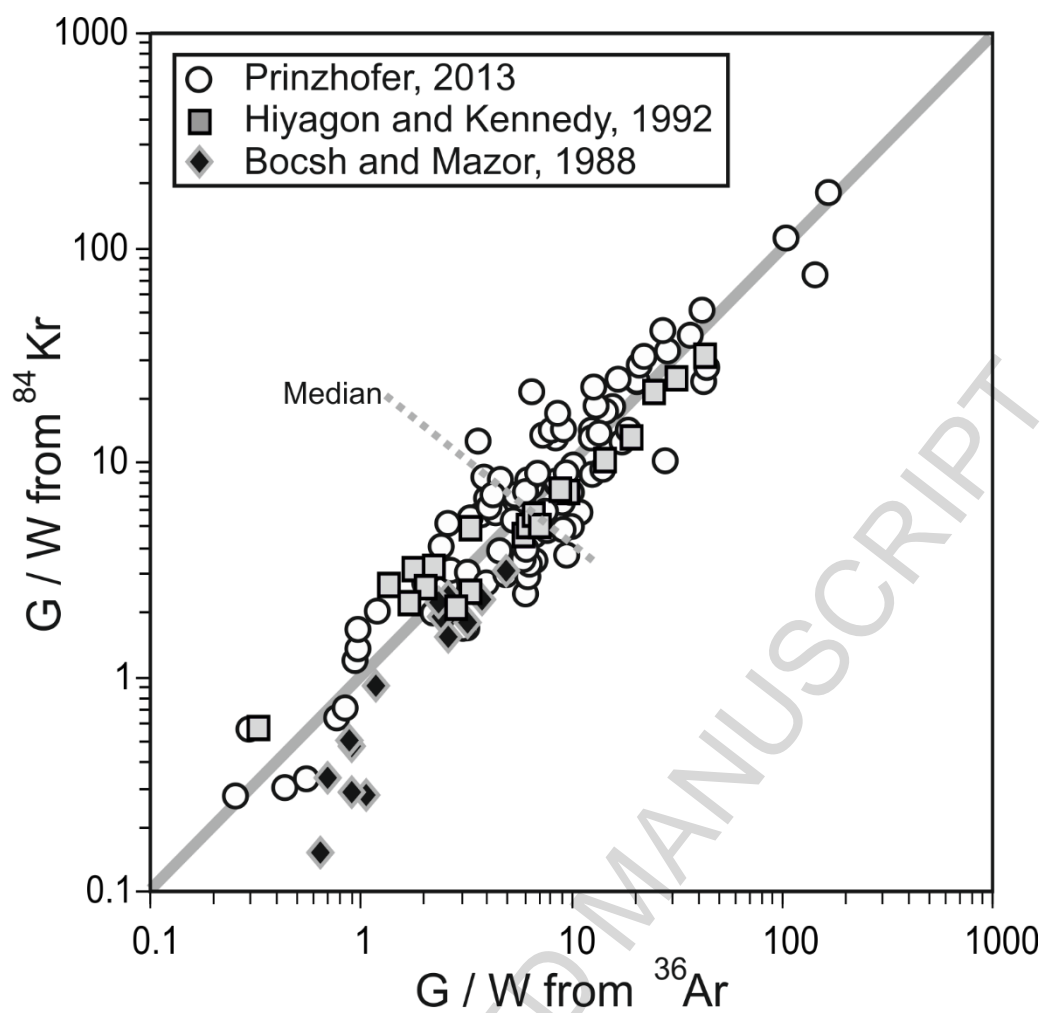
The apparent regression lines passing through zero could originate either from mixing of noble gases and hydrocarbons, or from different partial loss of noble gases. Grey square and diamond show assumed “end-member” concentrations. Extremely high concentrations of radiogenic species in the samples require meaningless accumulation time scales, exceeding the earth’s age (see Text).

However, substituting $^{21}\text{Ne}^*/^{21}\text{Ne}_{\text{AIR}}$ and $^{40}\text{Ar}^*/^{40}\text{Ar}_{\text{AIR}}$ ratios (seen as slopes of the regression lines) as well as $^4\text{He}^*/^{20}\text{Ne}$ from the above paper in Eqns (2, 4, or similar one adopted for $^{21}\text{Ne}^*$), give

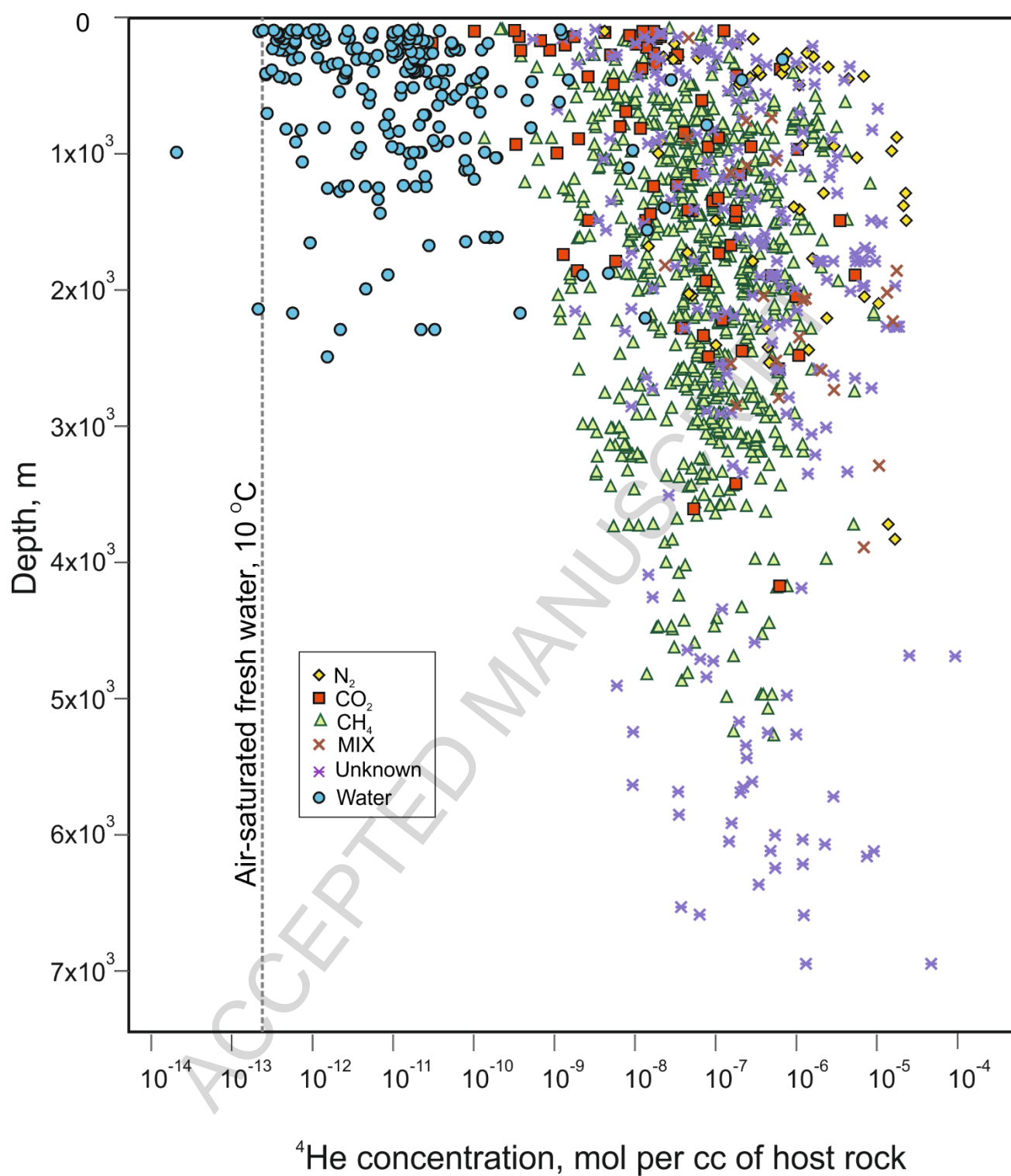
reasonable recharge – hydrocarbon contact intervals ≈ 500 Ma, approaching the stratigraphic ages of Brazilian sediments (Milani and Zalan, 1999).

ACCEPTED MANUSCRIPT

ACCEPTED MANUSCRIPT

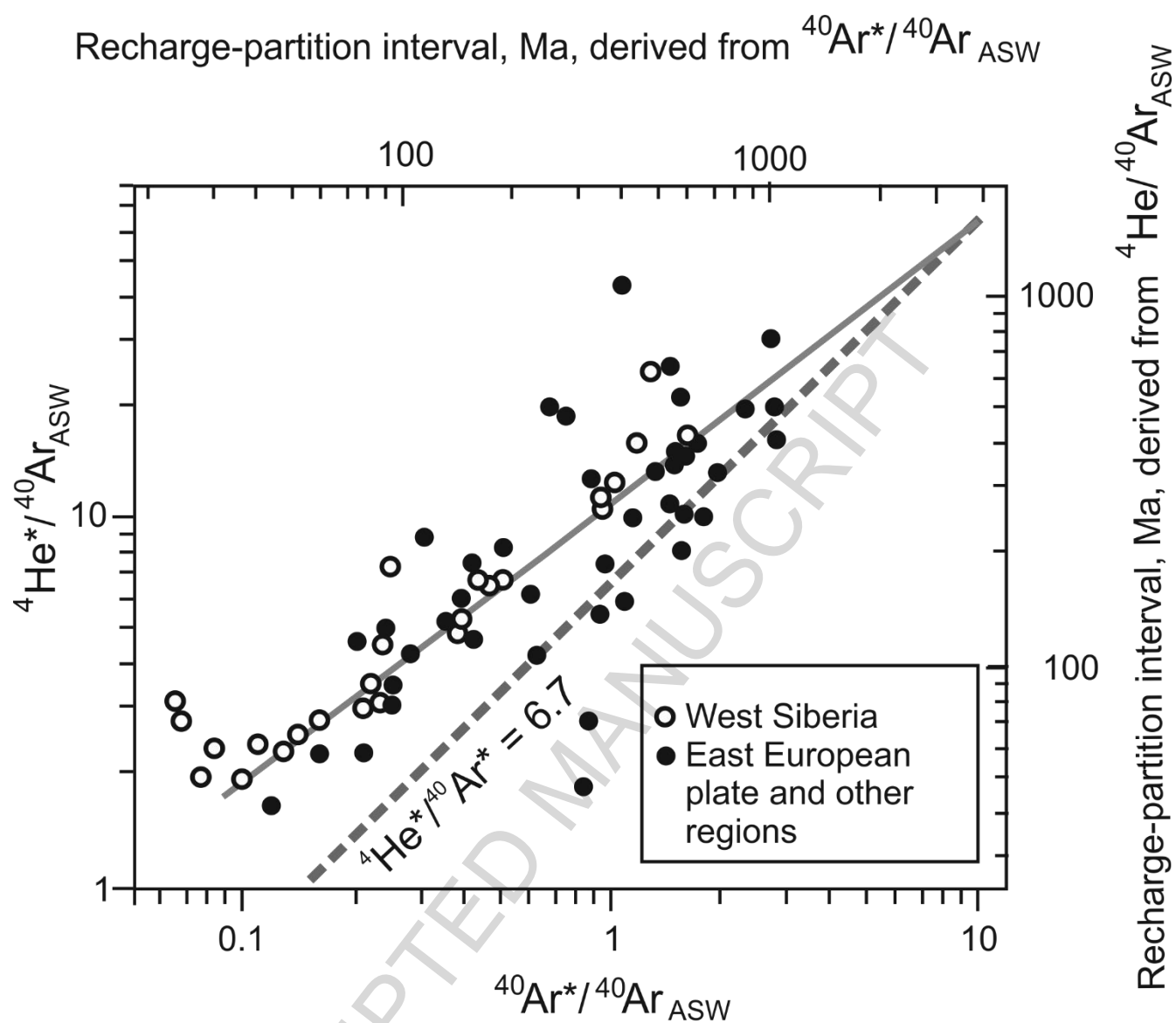


CHEMGE10355 Fig. 1, Tolstikhin et al., "Noble gas isotope record ... "

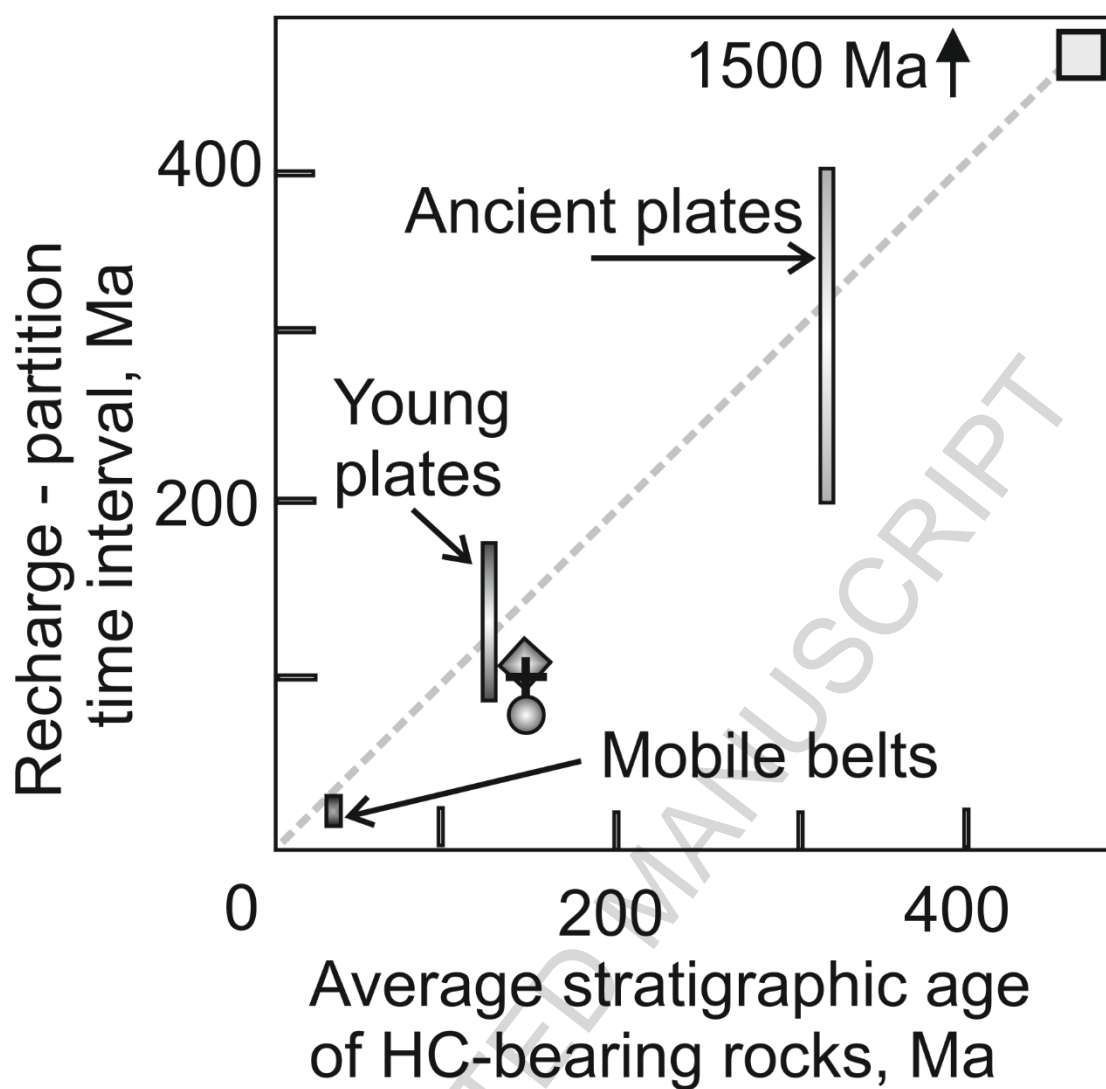


CHEMGE10355 Fig. 2, Tolstikhin et al., "Noble gas isotope record ... "

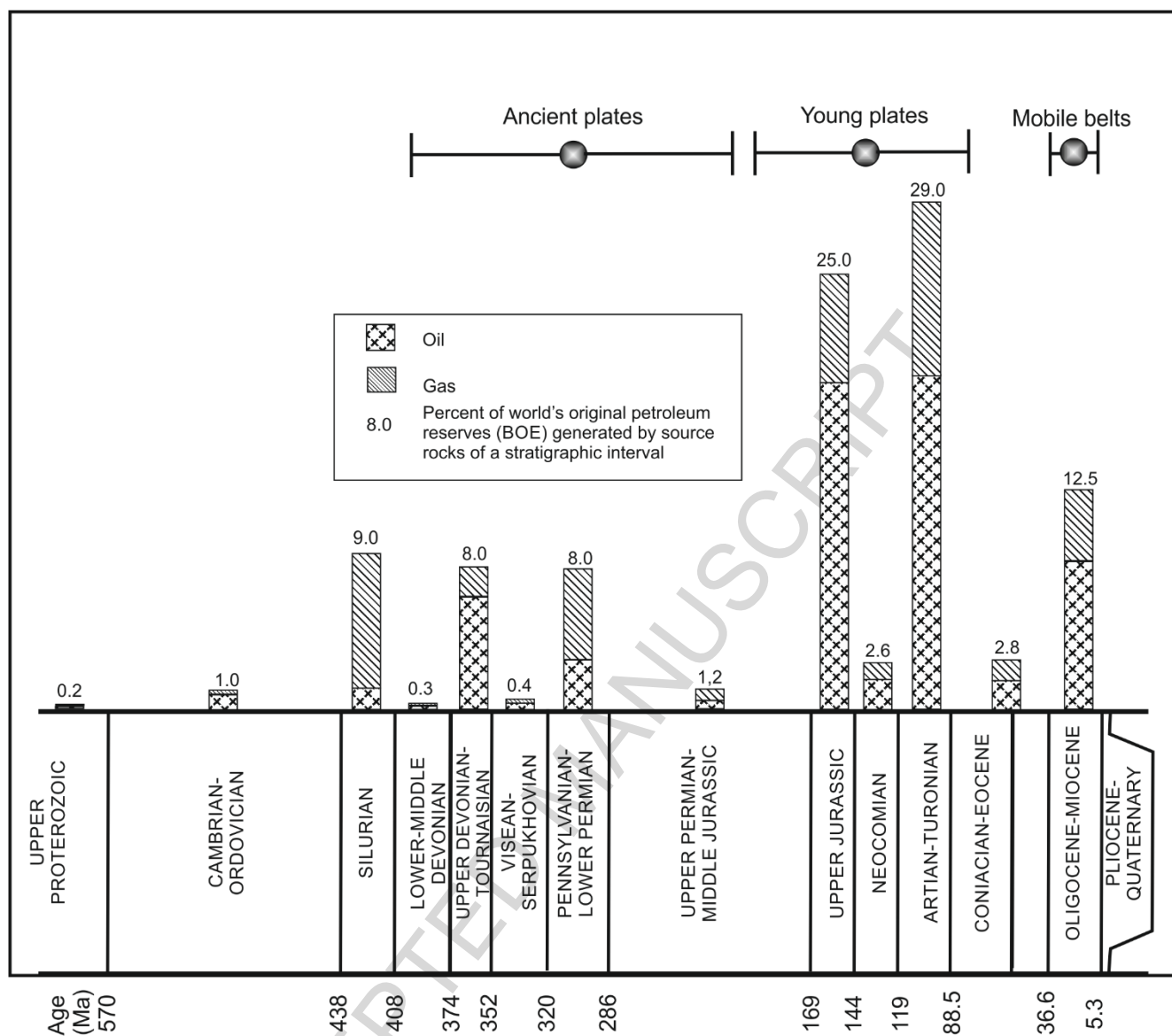
ACCEPTED MANUSCRIPT



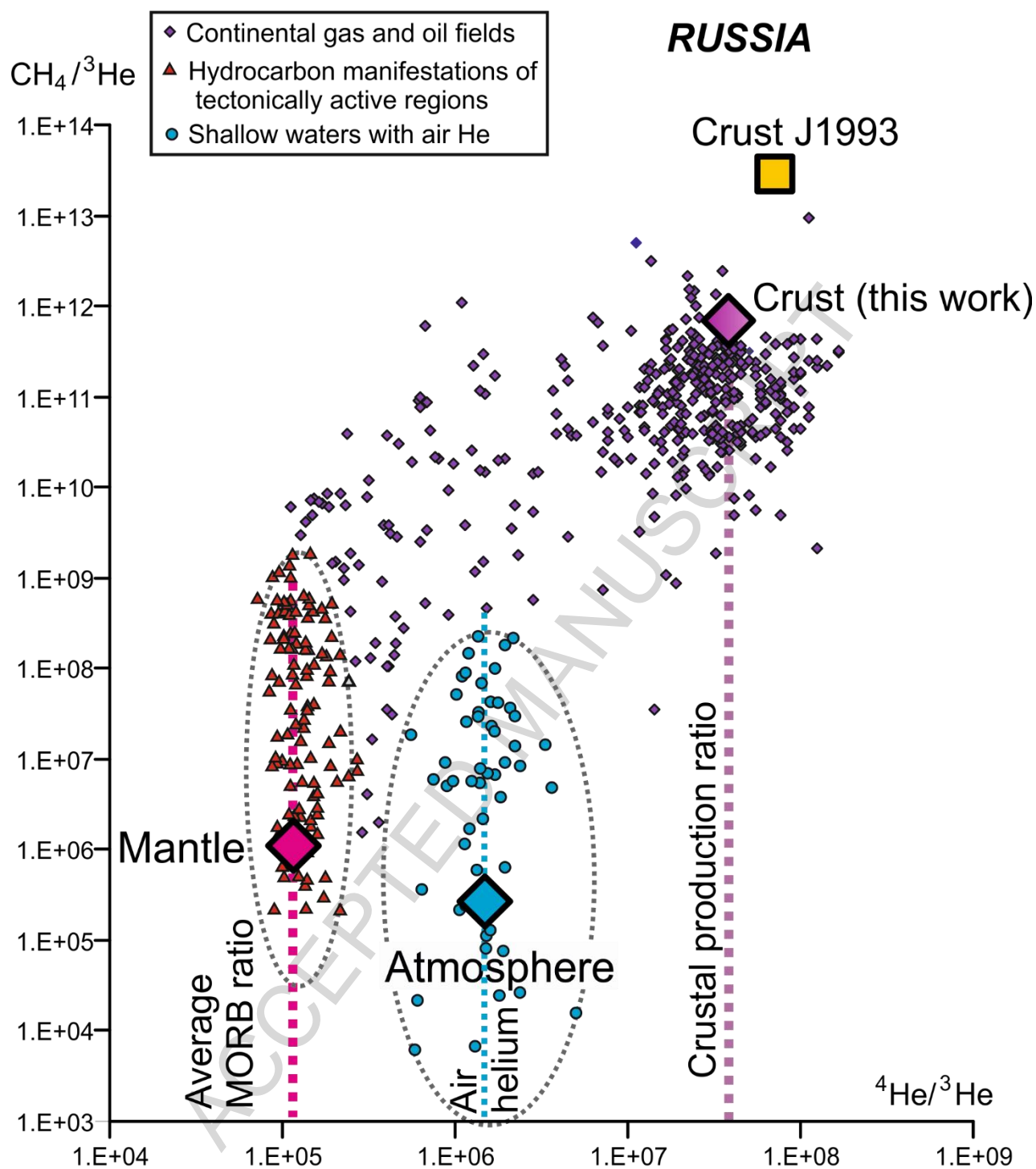
CHEMGE10355 Fig. 3, Tolstikhin et al., "Noble gas isotope record ... "



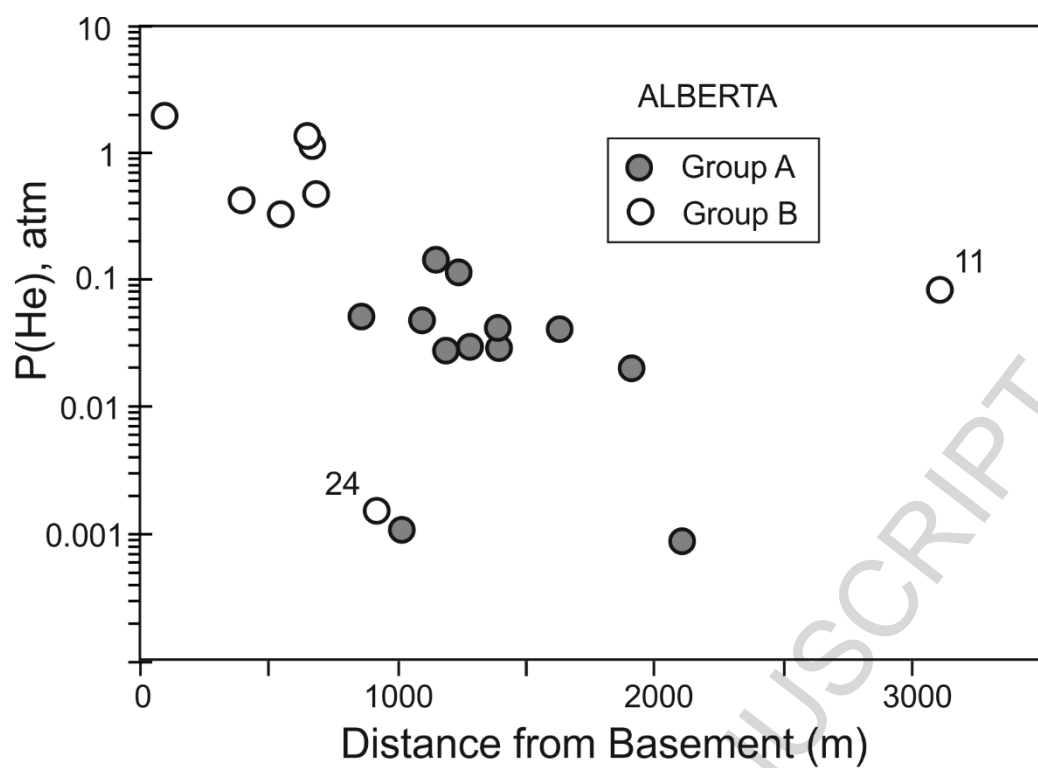
CHEMGE10355 Fig. 4, Tolstikhin et al., "Noble gas isotope record ... "



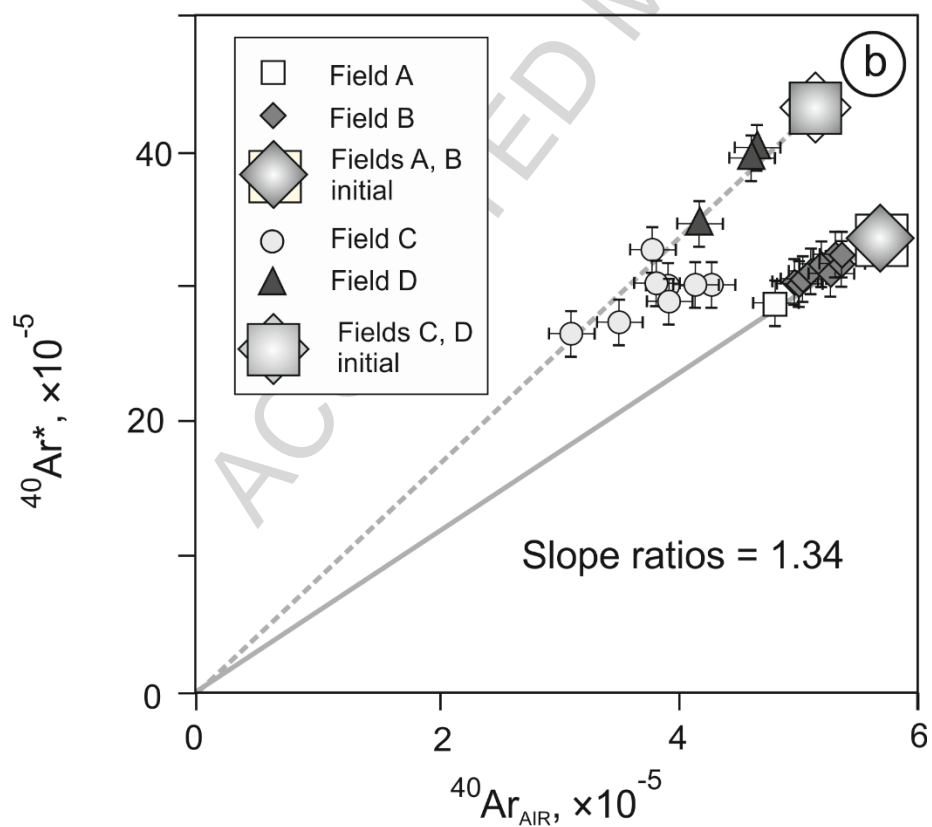
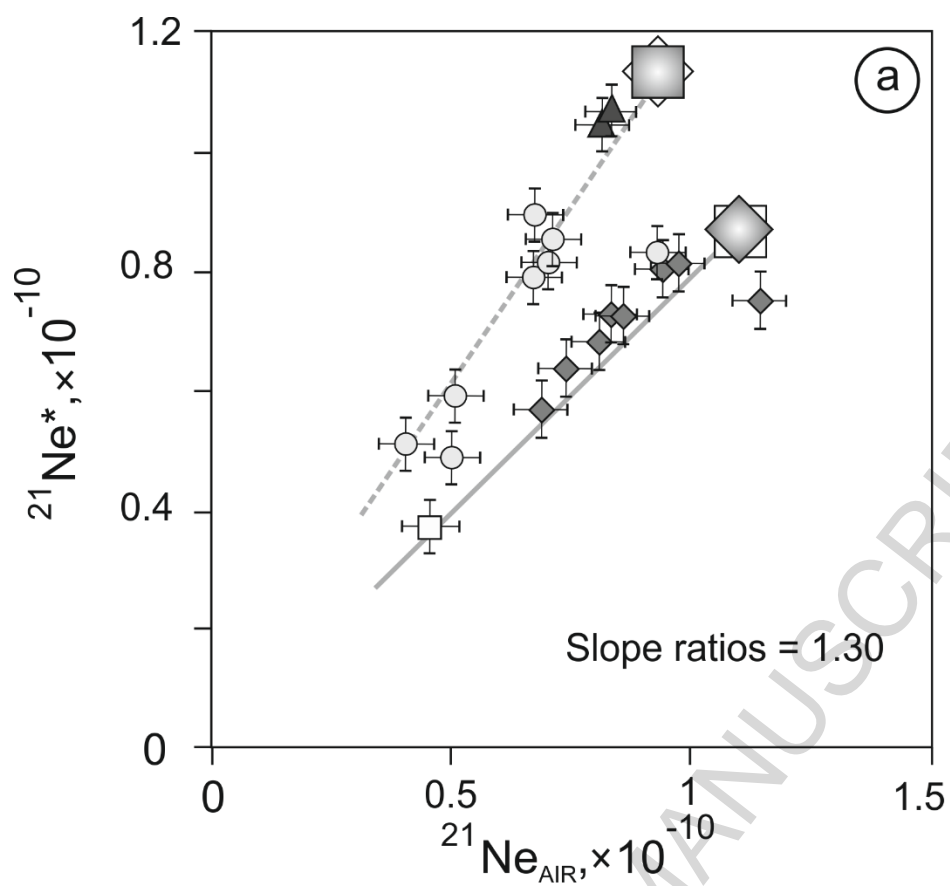
CHEMGE10355 Fig. 5, Tolstikhin et al., "Noble gas isotope record ... "



CHEMGE10355 Fig. 6, Tolstikhin et al., "Noble gas isotope record ... "



CHEMGE10355 Fig. 7, Tolstikhin et al., "Noble gas isotope record ... "



ACCEPTED MANUSCRIPT

Table 1. Noble gas abundances, the average stratigraphic ages, durations of recharge - partition time intervals (RPTI) and U-Th-He accumulation ages for the “average” hydrocarbon fields in different tectonic settings.

Tectonic Setting	$^{40}\text{Ar}_{\text{AIR}}$		$^4\text{He}^*$		$^4\text{He}^*/^{40}\text{Ar}_{\text{ASW}}$		$^{40}\text{Ar}^*/^{40}\text{Ar}_{\text{ASW}}$		$^4\text{He}^*/^{40}\text{Ar}^*$		Stratigraphic age ^b		RPTI ^c	$^4\text{He}^*$ ^d	U-Th-He ^e
	N ^a	$\times 10^{-5}$	N ^a		N ^a	Ratio	N ^a	Ratio	N ^a	Ratio	N ^a	Ma	Ma	mol cm ⁻³	Ma
1	2	3	4	5	6	7	8	9	10	11	12	13	14	15	16
Ancient plates	121	3.7	1306	1.2×10^{-3}	133	16	134	1.0	159	19	149	320	300	1.4×10^{-6}	6300
Young plates	827	2.7	641	2.9×10^{-4}	134	6.5	132	0.72	198	8.9	164	130	120	3.3×10^{-7}	3300
Mobile belts	322	2.2	38	2.0×10^{-5}	20	1.1	38	0.23	30	4.2	28	35	22	2.3×10^{-8}	300

Footnotes to Table:

^a N shows number of hydrocarbon fields, for which the average value is given in the next column.

^b The average age of host rocks, bearing hydrocarbon accumulations in different tectonic settings: Cenozoic **mobile belts** (e.g., Kamchatka, Sakhalin, Japan); **young** (post-Hercynian) **plates** (e.g., Turan, Scythian, West-Siberian); **ancient** (Precambrian) **plates** (e.g., East European, East Siberian).

^c Time interval between ground water recharge and noble gas partitioning between water and hydrocarbon materials. To calculate the intervals we use $^4\text{He}^*/^{40}\text{Ar}_{\text{ASW}}$, $^{40}\text{Ar}^*/^{40}\text{Ar}_{\text{ASW}}$, $^4\text{He}^*/^{20}\text{Ne}_{\text{ASW}}$, and $^{21}\text{Ne}^*/^{21}\text{Ne}_{\text{ASW}}$ ratios (Eqns 2 and 4) and apply the following parameters: the average crustal $U = 2.7 \text{ g g}^{-1}$, $Th = 10.5 \text{ g g}^{-1}$, $K = 0.023 \text{ g g}^{-1}$ (Rudnick and Gao, 2003); the production ratio of $^4\text{He}^*/^{21}\text{Ne}^* = 2.2 \times 10^7$ (Porcelliu et al., 2002); the water-bearing rock density 2.7 g cm^{-3} ; the porosity 0.1; the loss parameters: $L_4 = 1.0$, $L_{40} = 0.5$, 0.7, 1.0 for the ancient plates, young plates and mobile belts, respectively, $L_{21} = 0.75$; the concentrations of $^{20}\text{Ne}_{\text{ASW}} = 8.5 \times 10^{-12} \text{ mol cc}^{-1} \text{ H}_2\text{O}$; $^{40}\text{Ar}_{\text{ASW}} = 1.7 \times 10^{-8} \text{ mol cc}^{-1}$ in 10°C fresh water (Peeters et al., 2002) and $^{40}\text{Ar}_{\text{ASW}} = 8.6 \times 10^{-9} \text{ mol cc}^{-1} \text{ H}_2\text{O}$ in 40°C sea water (Weiss, 1970). In column 14 we present the average RPTI values, calculated by using $^4\text{He}^*/^{40}\text{Ar}_{\text{ASW}}$ ratio for both, fresh and saline waters at recharge. Note a good correlation between RPTI values (col. 14) and the average stratigraphic ages (col. 13, see also text in Section 3.2).

^d $^4\text{He}^*$ concentrations in host rocks [mol cm^{-3}] were calculated by using the following parameters of the average hydrocarbon fields: $^4\text{He}^*$ concentrations from the Table (col. 5), depth 1500 m, temperature 45°C , host rock density 2.7 g cm^{-3} , porosity 0.2. Similar rather high ^4He concentrations can be derived for the “field conditions” from (i) the average partial pressure of $^{40}\text{Ar}_{\text{AIR}}$, 0.0034 atm (in 180 hydrocarbon fields, 0.003 to 0.0039 is a 95% confidence interval), corresponding to $^{40}\text{Ar}_{\text{AIR}} \approx 2.7 \times 10^{-8} \text{ mol cm}^{-3}$, and (ii) $^4\text{He}^*/^{40}\text{Ar}_{\text{AIR}}$ ratio in column 7. This approach gives $^4\text{He}^*$ concentrations in host rocks [mol cm^{-3}] 4.5×10^{-7} , 1.7×10^{-7} and 2.9×10^{-8} for the ancient plates, young plates and mobile belts, respectively.

^e Apparent U-Th-He “accumulation ages” obtained via substitution of ^4He concentrations from column 15 along with the average crustal concentrations of U and Th in Eqn 1b; meaningless values (much exceeding the stratigraphic ages) indicate a negligible contribution of in-situ produced radiogenic ^4He in the rock - pore fluid system of hydrocarbon fields. This is also valid for $^4\text{He}^*$ amounts obtained via partial pressure of $^{40}\text{Ar}_{\text{AIR}}$ (see Footnote ^d): the corresponding apparent accumulation ages are [Ma] 4000, 2100 and 380 for the ancient plates, young plates and mobile belts, respectively. The K-Ar “accumulation ages”, obtained by using $^4\text{He}^*$ concentrations (col. 15) and $^4\text{He}^* / ^{40}\text{Ar}^*$ ratios (col. 11) from the Table 1 along with the average crustal K are 6700, 2000 and 490 Ma for the fields situated in the ancient plates, young plates and mobile belts, respectively. Similar meaningless accumulation ages result from $^{40}\text{Ar}^*$ concentrations, obtained from $^{40}\text{Ar}_{\text{AIR}}$ (col. 3) and $^{40}\text{Ar}^* / ^{40}\text{Ar}_{\text{ASW}}$ (col. 9).

Sources of data to Table 1: Ballentine et al. (1991), Ballentine and O’Nions (1992), Dai et al. (2008), Elliot et al. (1993), Gavrilov et al. (1972), Gavrilov and Teplinskiy (1973), Gerling et al. (1967), Jin et al. (2009), Jenden et al. (1993), Kamensky et al. (1974), Lobkov and Prasolov (1976), Marty (1995), Nagao et al. (1981), Nesmelova et al. (1975), Nesterov et al. (1976), Ni et al. (2014), Prasolov et al. (1980), Prasolov (1981, 1990), Prasolov et al. (1981), Prasolov et al. (1987), Prinzhofer et al. (2010), Voronov and Prasolov (1974), Voronov et al. (1974), Xu et al. (1995a, 1995b, 1982).